CIGRE Generalforsamling Aalborg 2026

Blackstart of de-energised Offshore Wind Power Plants after a Blackout

Leonel Noris

Why offshore wind blackstart?

IBR Blackout Recovery

- **Blackout**—Unplanned, widespread loss of electricity supply.
- The affected network loses voltage and a usable frequency reference.
- **Adverse Impacts**
  - Human Safety
  - Critical Services
  - Economic Losses
  - Grid Equipment Damage
  - Social Disruption
  - Cascading Failure to other Infrastructures
- **Coal and Gas Power Plants phase out—**As conventional blackstart providers retire, renewable alternatives are needed.
- Need to develop Blackstart solutions based on Renewables.





Recent Blackouts			
	Location	Date	People Affected (Millions)
1	Spain & Portugal	2025	≈ 60
2	Venezuela	2024	≈ 20
3	Lebanon	2024	≈ 6
4	South Africa	2024	≈ 60
5	Pakistan	2023	≈ 220
6	Bangladesh	2022	≈ 140
7	Australia	2016	≈ 2
8	India	2012	≈ 620



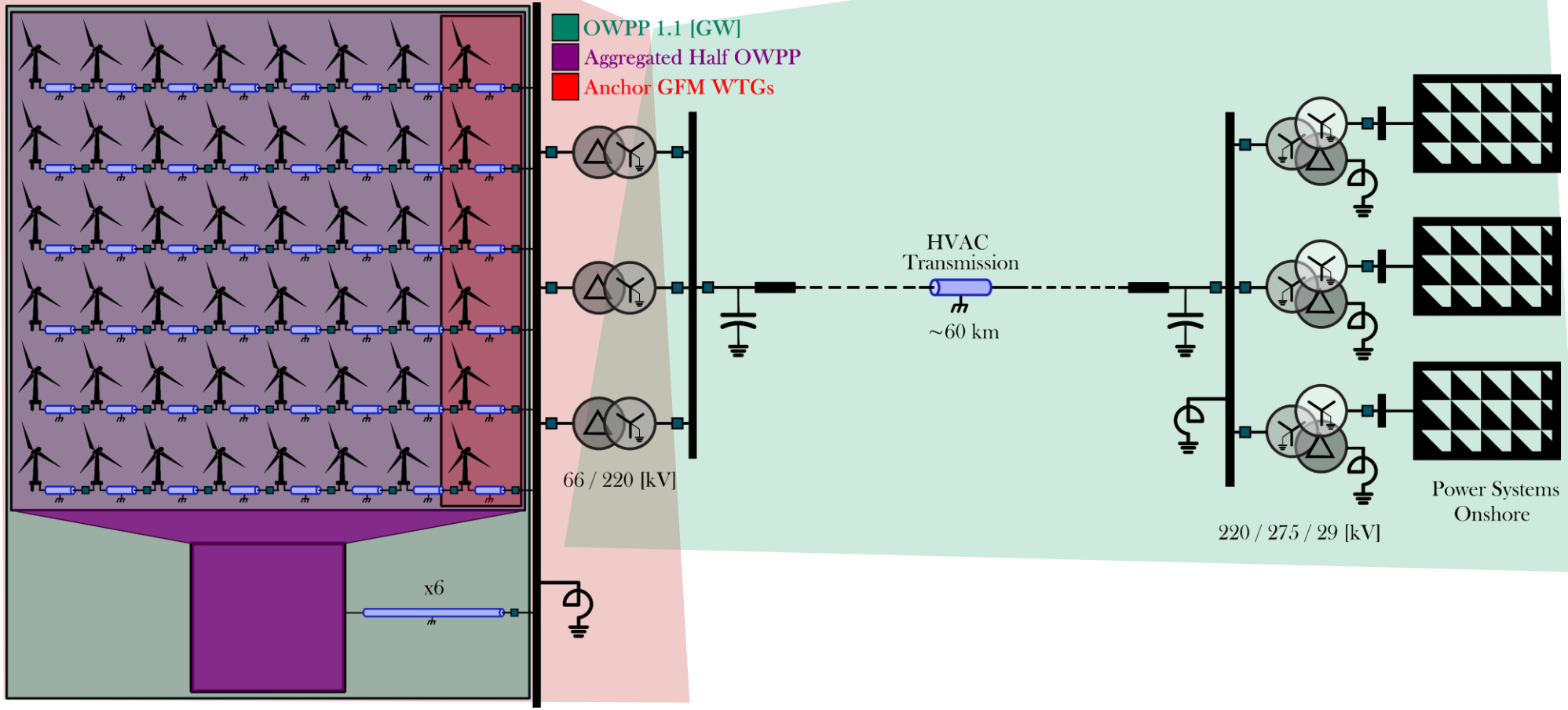
[1]

OWPP blackstart and system restoration

Stage 1: OWPP island formation—Stage 2: power grid recovery

Stage 1: OWPP Blackstart (Island Operation)

Stage 2: System Restoration



Stage 1: OWPP Blackstart (Island Operation)

a) Self-start GFM anchors and supply auxiliaries.
b) Establish v_{AC} and f and energise collector strings.
c) Connect GFL WTGs and stabilise the island.

Stage 2: System Restoration

a) Energise HV transformers and export cables.
b) Restore onshore substations and pick up loads.
c) Expand the island and synchronise with neighbouring networks.

[2]

Research questions: OWPP Blackstart

Stage 1: self-start and collector recovery

Research Questions	KPIs
1. Under what wind and initial energy conditions can the anchor WTG self-start and sustain the operation?	Rotor speed, DC voltage, startup time and energy balance.
2. How can the anchor energise the collector within voltage and current limits?	Hard versus soft energisation, voltage and current peaks.
3. How can followers join and share power without destabilising the island?	Connection sequence, power sharing, converter and network interactions.

Sensitivity cases: wind variability, cable layout and GFM number/placement.

Self-Starting Anchor GFM WTG

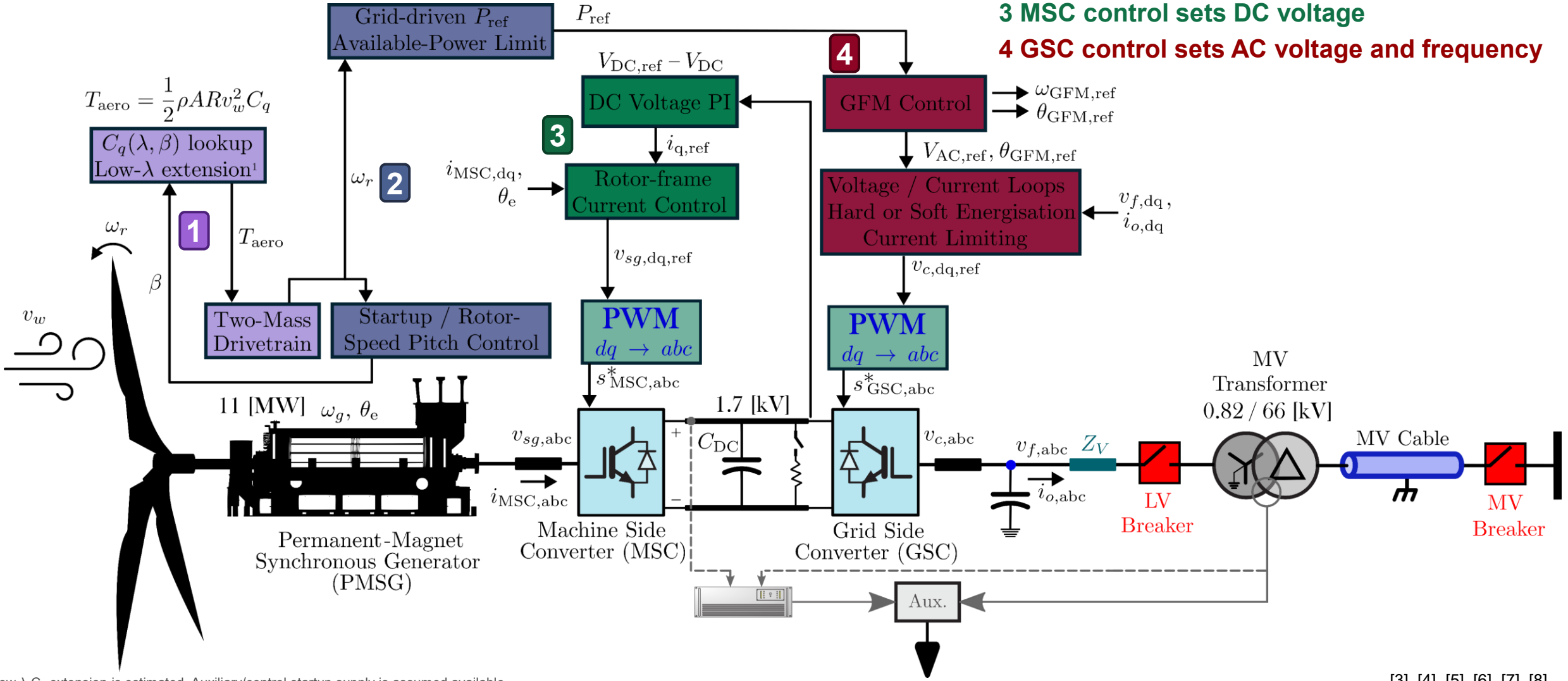
Modifications for self-start GFM WTG

1 Wind produces starting torque

2 Coordinate power, pitch and speed

3 MSC control sets DC voltage

4 GSC control sets AC voltage and frequency



[1] Low-λ C_q extension is estimated. Auxiliary/control startup supply is assumed available.

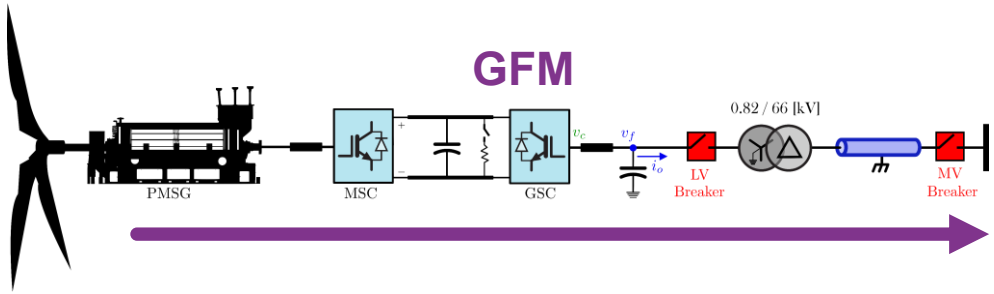
[3], [4], [5], [6], [7], [8]

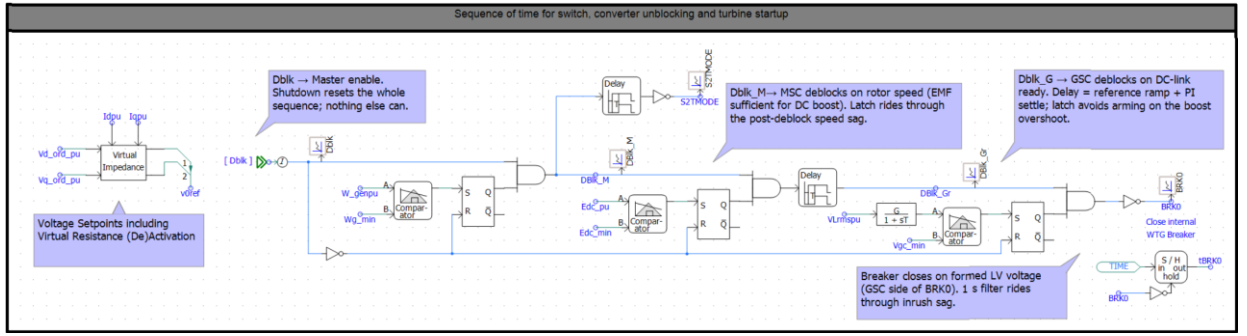
GFM and GFL WTG startup sequences

Readiness checks and converter deblocking

Anchor GFM WTG

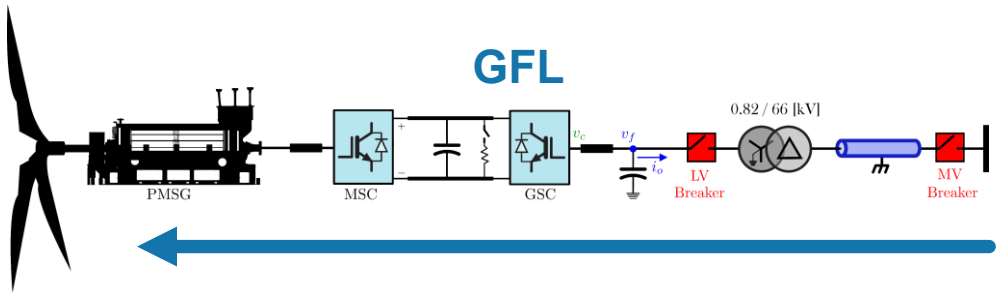
1	2	3	4	5
Wind + auxiliaries ready **Rotor accelerates**	Rotor / EMF ready **Deblock MSC controls**	DC voltage ready **Deblock GSC controls**	LV voltage established **Close LV breaker**	Collector energisation **Supply the string**

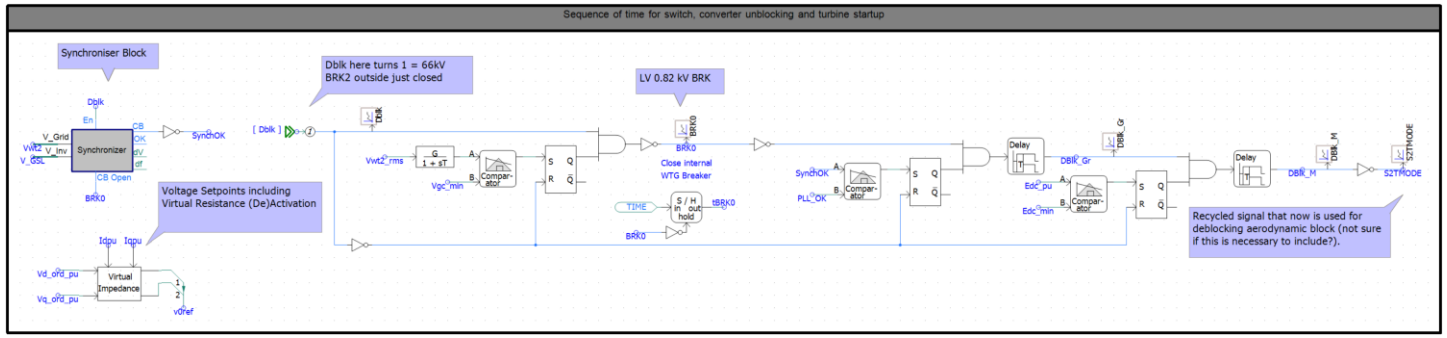




Follower GFL WTG

1	2	3	4	5
MV breaker closed **Enable startup**	LV voltage ready **Close LV breaker**	PLL Synchronisation ready **Deblock GSC controls**	DC voltage ready **Deblock MSC controls**	Converters operational **Contribute power**

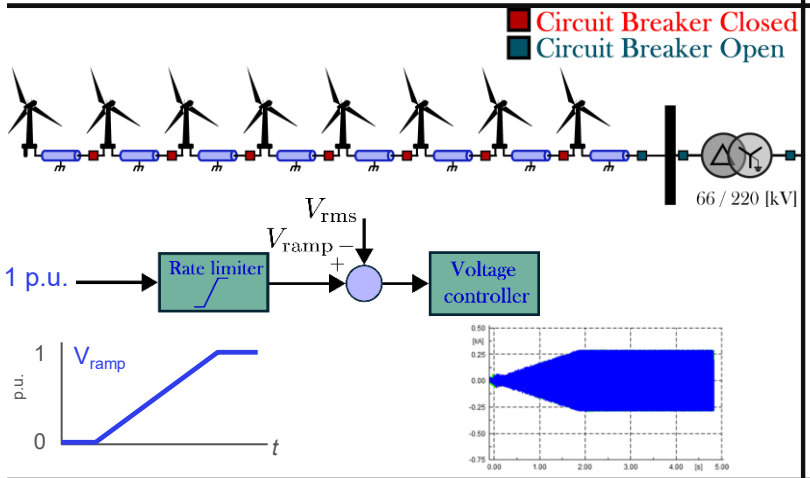




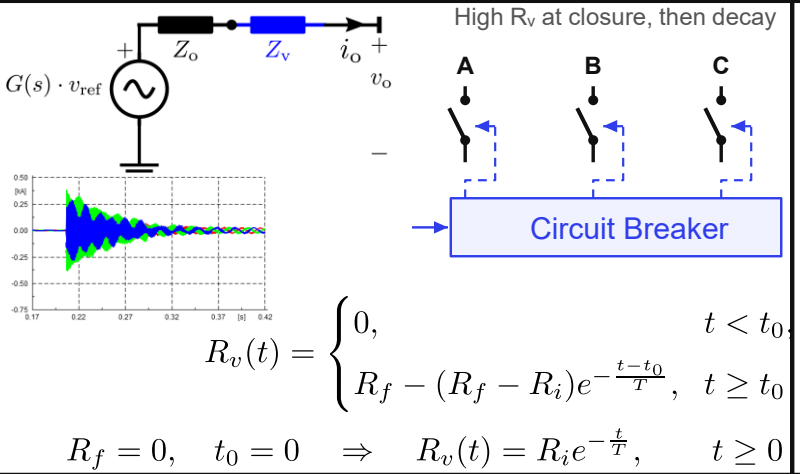
Soft and hard energisation

Voltage Ramping, Virtual Resistance R_V and Point-On-Wave POW Switching

Soft Energisation



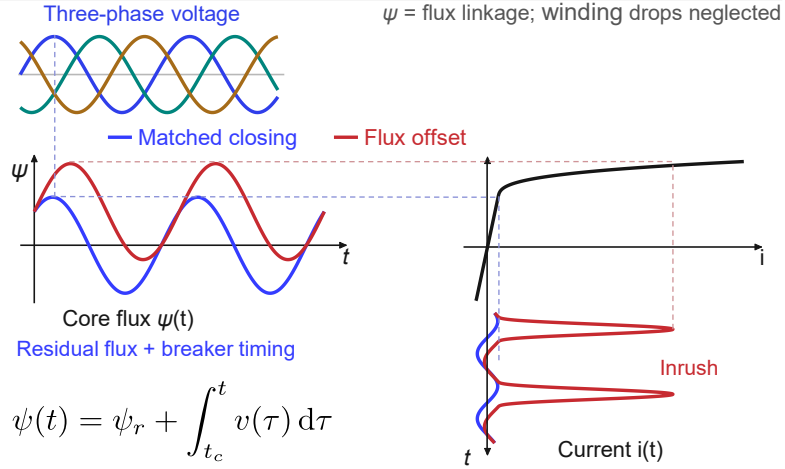
Hard Energisation R_V



$$R_v(t) = \begin{cases} 0, & t < t_0 \\ R_f - (R_f - R_i)e^{-\frac{t-t_0}{T}}, & t \geq t_0 \end{cases}$$

$$R_f = 0, \quad t_0 = 0 \quad \Rightarrow \quad R_v(t) = R_i e^{-\frac{t}{T}}, \qquad t \geq 0$$

Hard Energisation POW



$$\psi(t) = \psi_r + \int_{t_c}^{t} v(\tau)\,\mathrm{d}\tau$$

Soft Energisation	Hard Energisation R_V	Hard Energisation POW
Mechanism Connect the dead section before applying voltage. Ramp the GFM voltage from 0 to 1 p.u.	**Mechanism** The converter emulates resistance by adjusting its voltage reference in proportion to current.	**Mechanism** Select the closing instant so the target flux matches the residual flux, minimising flux offset and saturation.
Advantages Lower inrush and voltage stress. Several assets energise together.	**Advantages** Limits inrush through converter control. Adjustable damping for each closure.	**Advantages** Reduces transformer inrush by limiting flux offset. Optimizes breaker closing timing for low inrush.
Limitations Low-voltage protection and auxiliaries. Residual flux may need conditioning.	**Limitations** Voltage depression in the live island. Coordinate current limits and DC control.	**Limitations** Residual-flux and timing uncertainty. Breaker calibration and commissioning.

All three require adequate P/Q capability and protection coordination. Cable charging remains at nominal voltage.

[9], [10], [11], [12], [13]

Single-string blackstart model

One GFM anchor and seven auxiliary-load equivalents

OWPP String Model

- Based on Seagreen OWPP in Scotland.
- Seagreen-based cable layout and distances [km].
- Selected eight-turbine string.

Anchor GFM Turbine

- Includes PMSG, Two-Mass Drivetrain and Aerodynamics.
- Grid-driven Pref follows string energisation demand.
- Three GFM modes were tested: Droop, VSM and PSC.

Non-generating WTGs

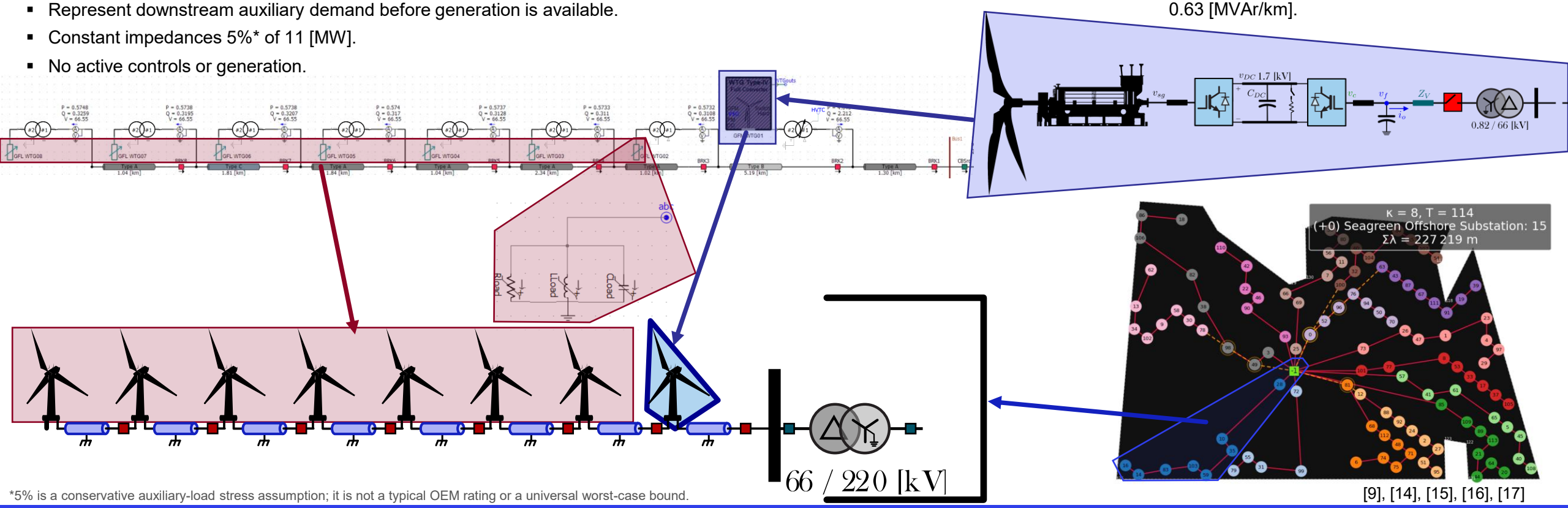
- Represent downstream auxiliary demand before generation is available.
- Constant impedances 5%* of 11 [MW].
- No active controls or generation.

0.82 / 66 [kV] Transformers

- High-frequency models.
- Saturation characteristics included.
- Hysteresis enabled.
- Iron and copper losses included.

66 [kV] Collector Cables

- Lumped π section model.
- Capacitive charging power of approx. 0.33 to 0.63 [MVAr/km].

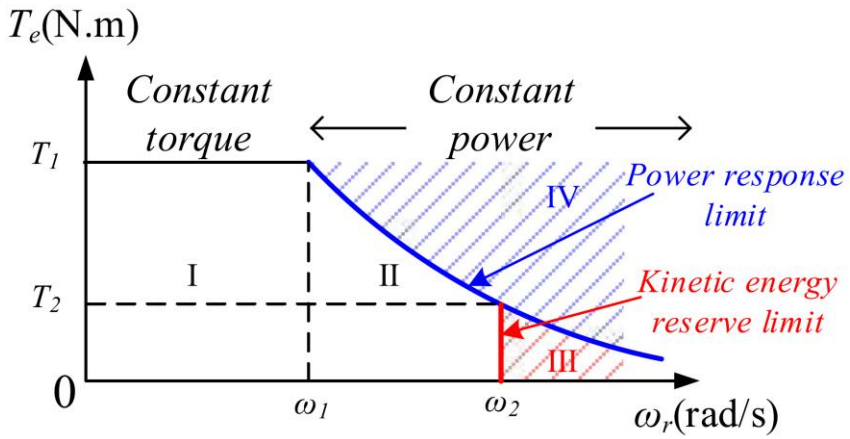


*5% is a conservative auxiliary-load stress assumption; it is not a typical OEM rating or a universal worst-case bound.

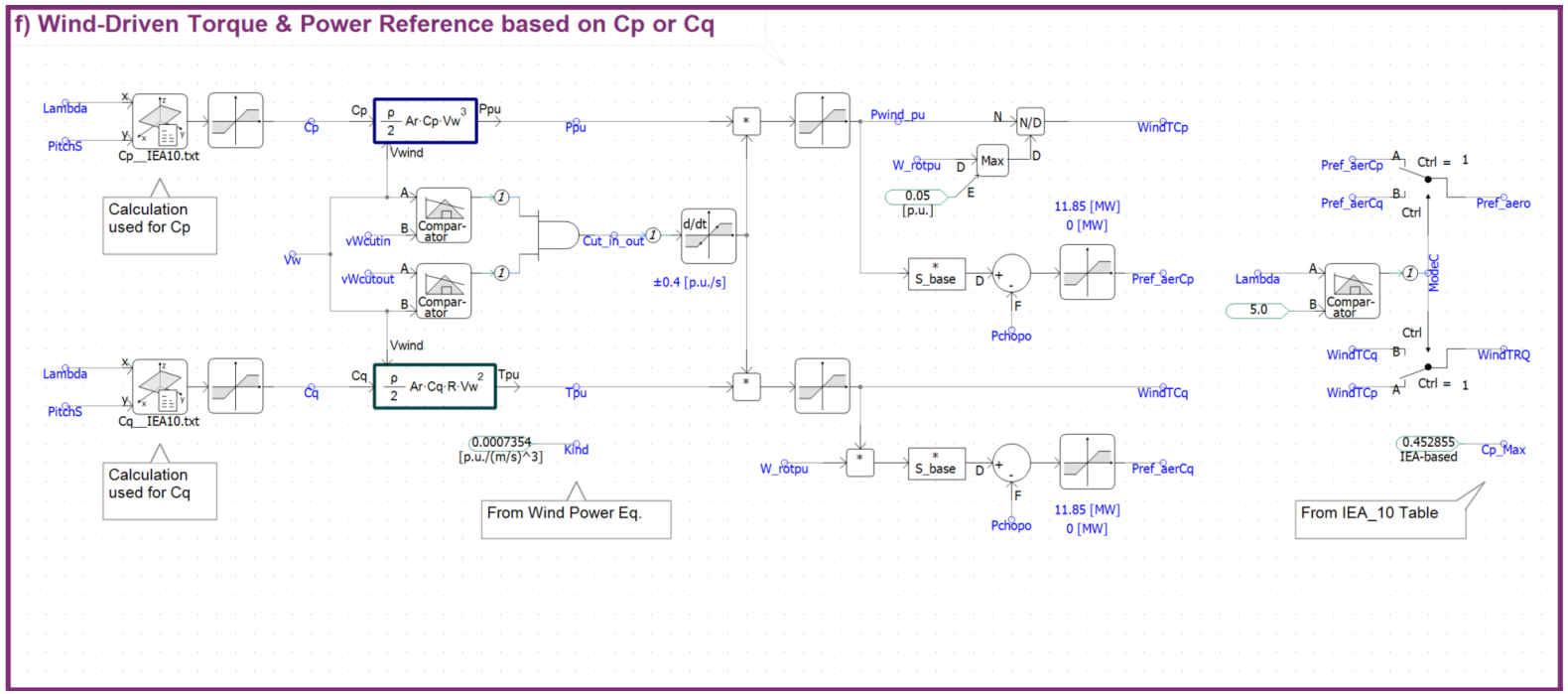
[9], [14], [15], [16], [17]

Wind-driven self-start model

Estimated torque characteristic at low tip-speed ratio



- Cq represents finite wind torque at standstill.
- An estimated low-λ Cq extension supplies finite starting torque.
- Acceleration requires aerodynamic torque to exceed opposing torque.
- Rotor and DC-link readiness trigger converter deblocking.
- Wind availability determines startup duration and kinetic-energy margin.
- Rotor energy reserves and converter current limits constrain power delivery during startup.



$$C_q(0,\beta) \equiv \lim_{\lambda \to 0^+} \frac{C_p(\lambda,\beta)}{\lambda}$$

$$T_{\text{aero}} = \frac{1}{2}\rho\pi R^3 v_w^2 C_q(\lambda,\beta)$$

$$P_{\text{aero,pu}} = T_{\text{aero,pu}}\,\omega_{\text{r,pu}}$$

$$J_{\text{eq}}\frac{\mathrm{d}\omega_{\text{r}}}{\mathrm{d}t} = T_{\text{aero}} - T_{\text{e}} - T_{\text{loss}}$$

$$T_{\text{e}} \approx 0, \qquad T_{\text{aero}} > T_{\text{loss}} \implies \frac{\mathrm{d}\omega_{\text{r}}}{\mathrm{d}t} > 0$$

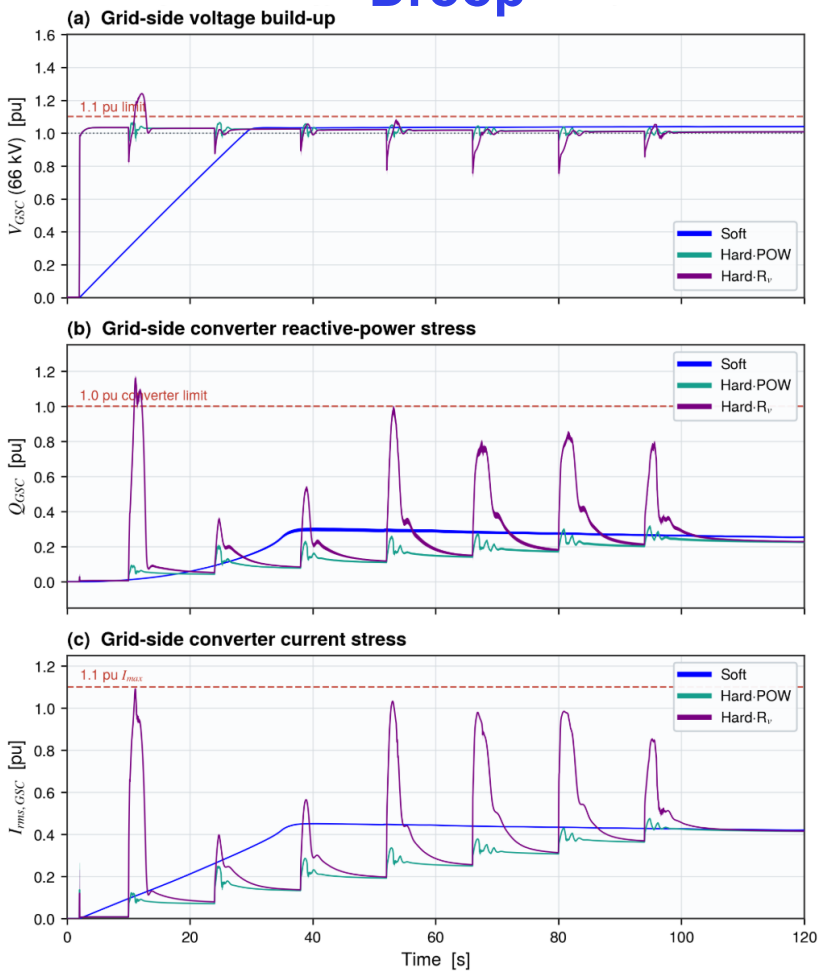
$$T_{\text{aero}} > 0 \implies \omega_{\text{r}} \uparrow \implies E_{\text{PMSG}} \uparrow \implies V_{\text{dc}} \uparrow \implies V_{\text{GSC}} \uparrow$$

[8], [10], [11], [13]

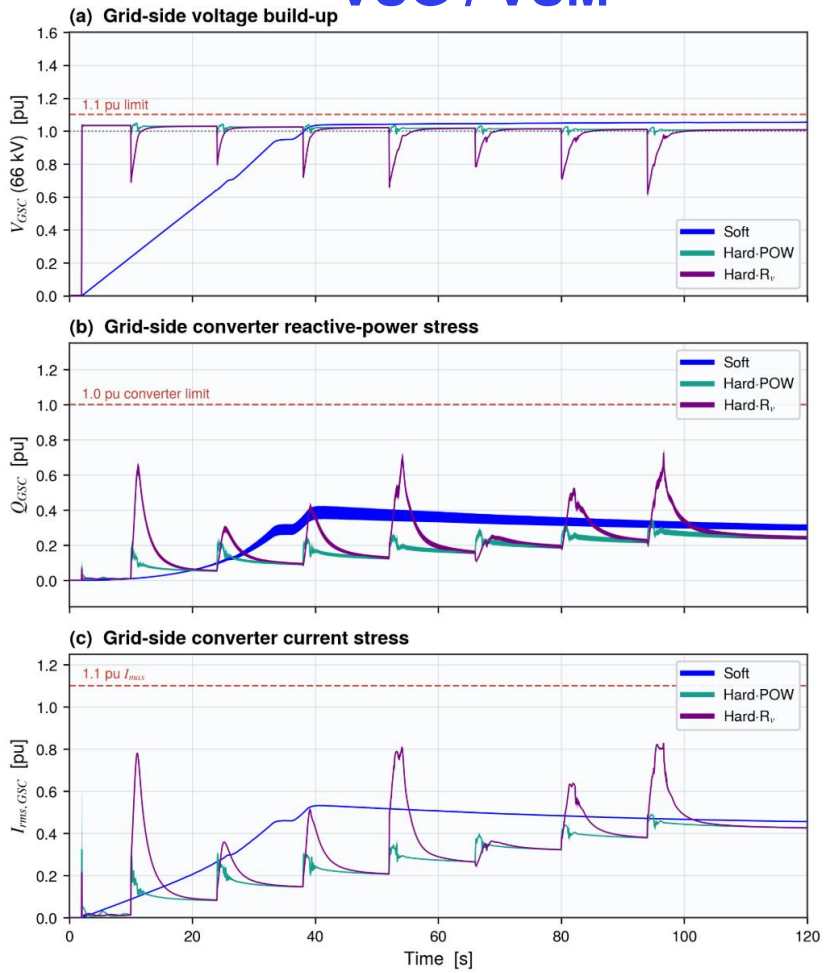
Collector energisation at 8 m/s—Passive Loads

Soft and hard energisation with GFM Droop, VSM and PSC

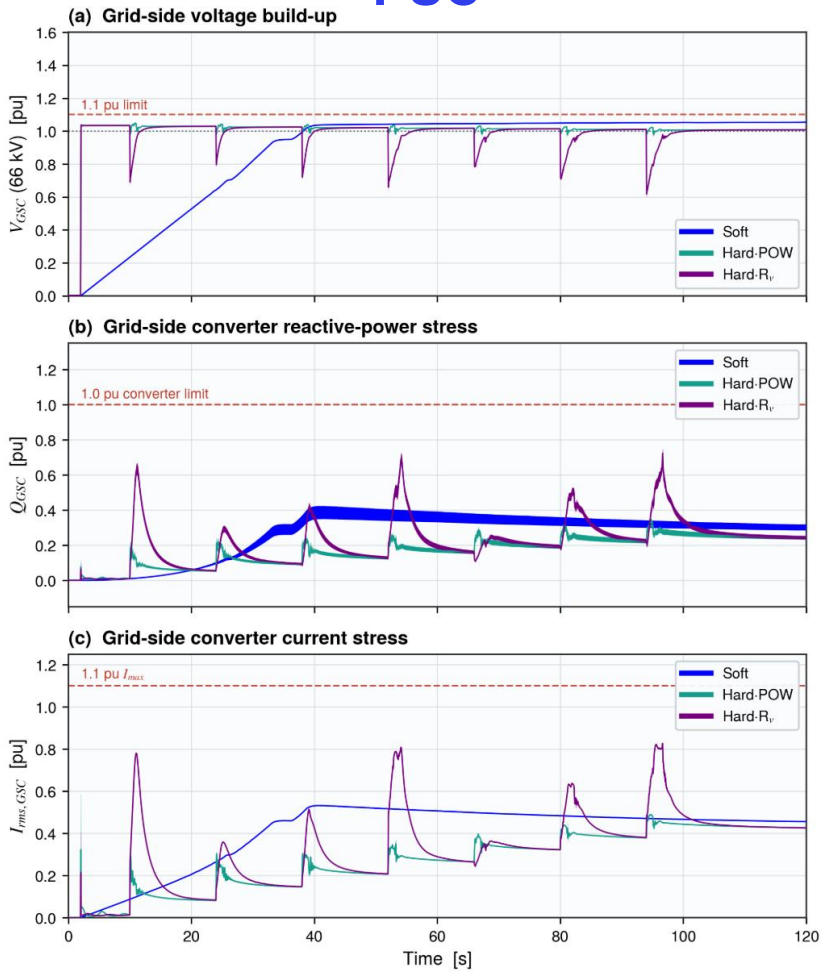
Droop



VSG / VSM

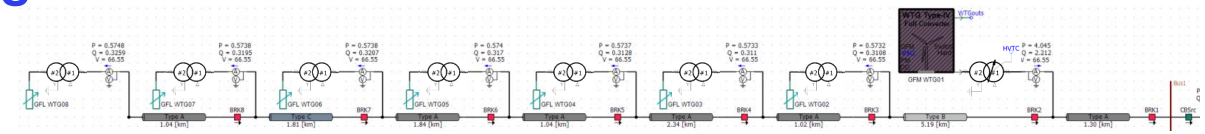


PSC

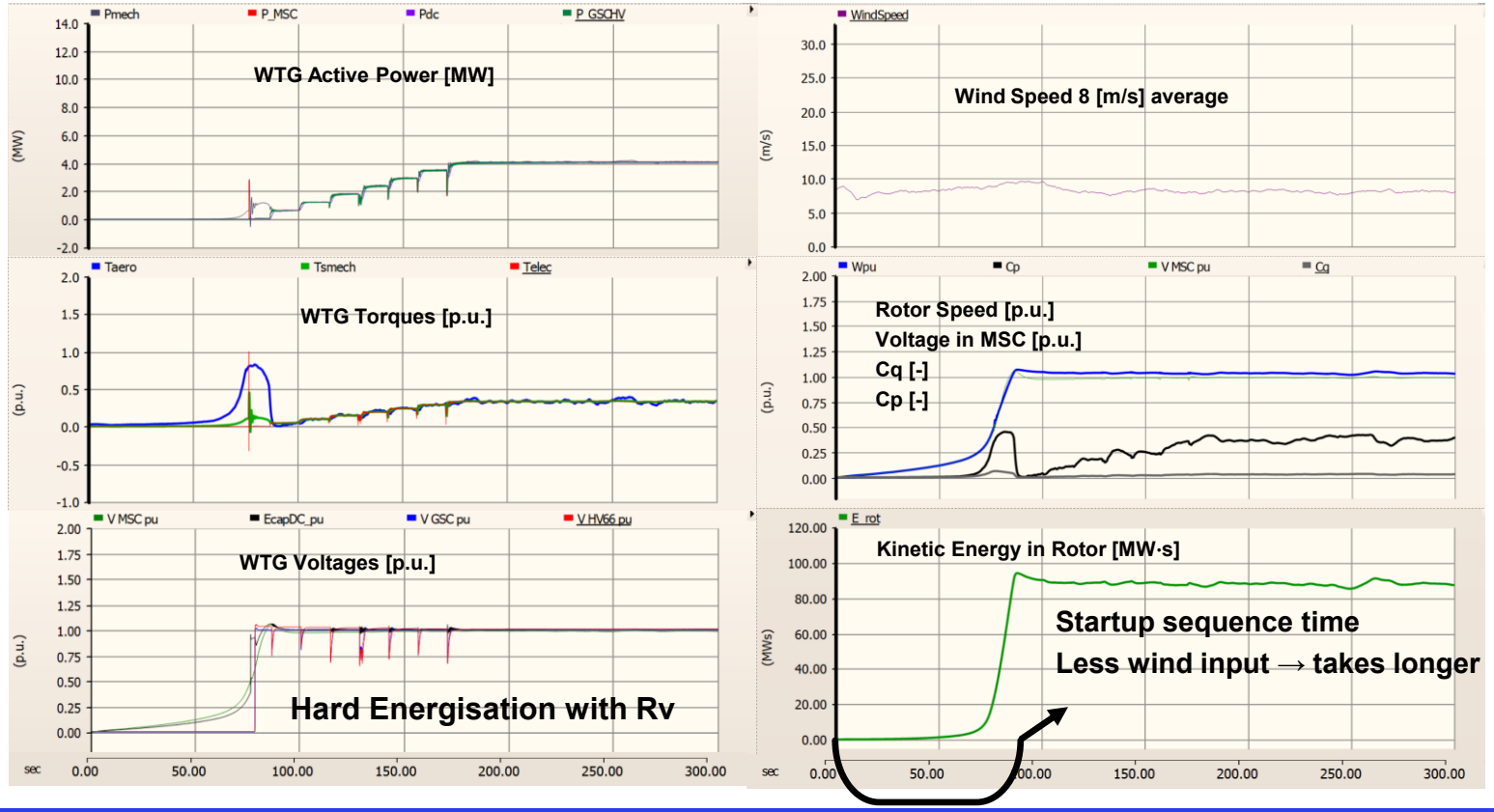


Anchor self-start at 8 m/s

Rotor and DC-link response with auxiliary loads



- One GFM anchor supplies seven 5% auxiliary-load equivalents.
- Hard Energisation Rv test successful; 8 m/s minimum wind→ lower wind string collapses.
- Rotor and DC-link readiness trigger converter deblocking.
- Staged load pickup reaches approximately 4 MW in the shown run.



$$C_q(0,\beta) \equiv \lim_{\lambda \to 0^+} \frac{C_p(\lambda,\beta)}{\lambda}$$

$$T_{\text{aero}} = \frac{1}{2}\rho\pi R^3 v_w^2 C_q(\lambda,\beta)$$

$$P_{\text{aero,pu}} = T_{\text{aero,pu}}\,\omega_{\text{r,pu}}$$

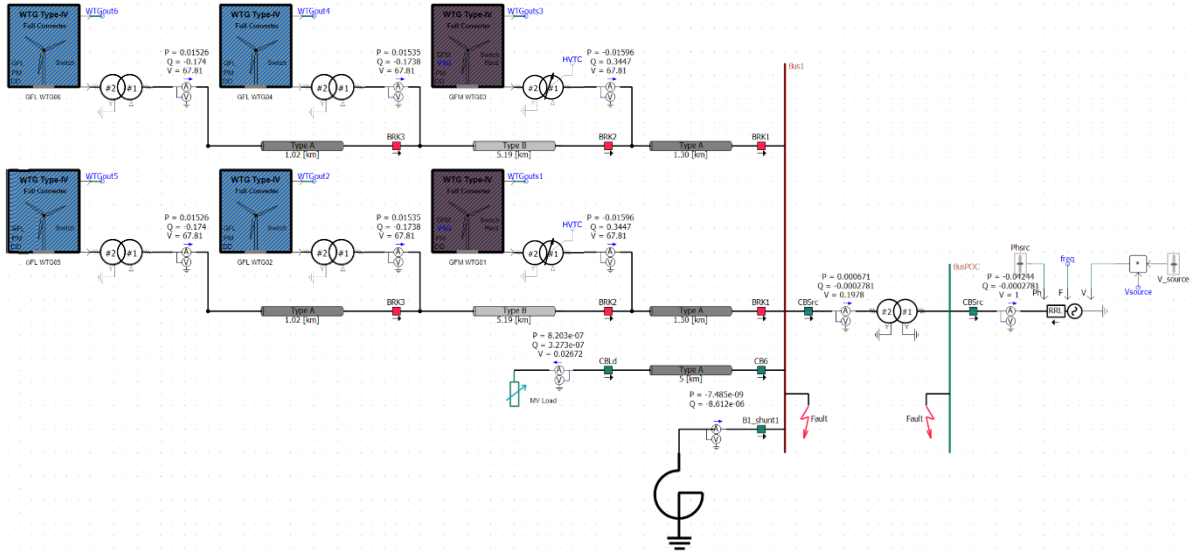
$$J_{\text{eq}}\frac{\mathrm{d}\omega_{\text{r}}}{\mathrm{d}t} = T_{\text{aero}} - T_{\text{e}} - T_{\text{loss}}$$

$$T_{\text{e}} \approx 0, \qquad T_{\text{aero}} > T_{\text{loss}} \implies \frac{\mathrm{d}\omega_{\text{r}}}{\mathrm{d}t} > 0$$

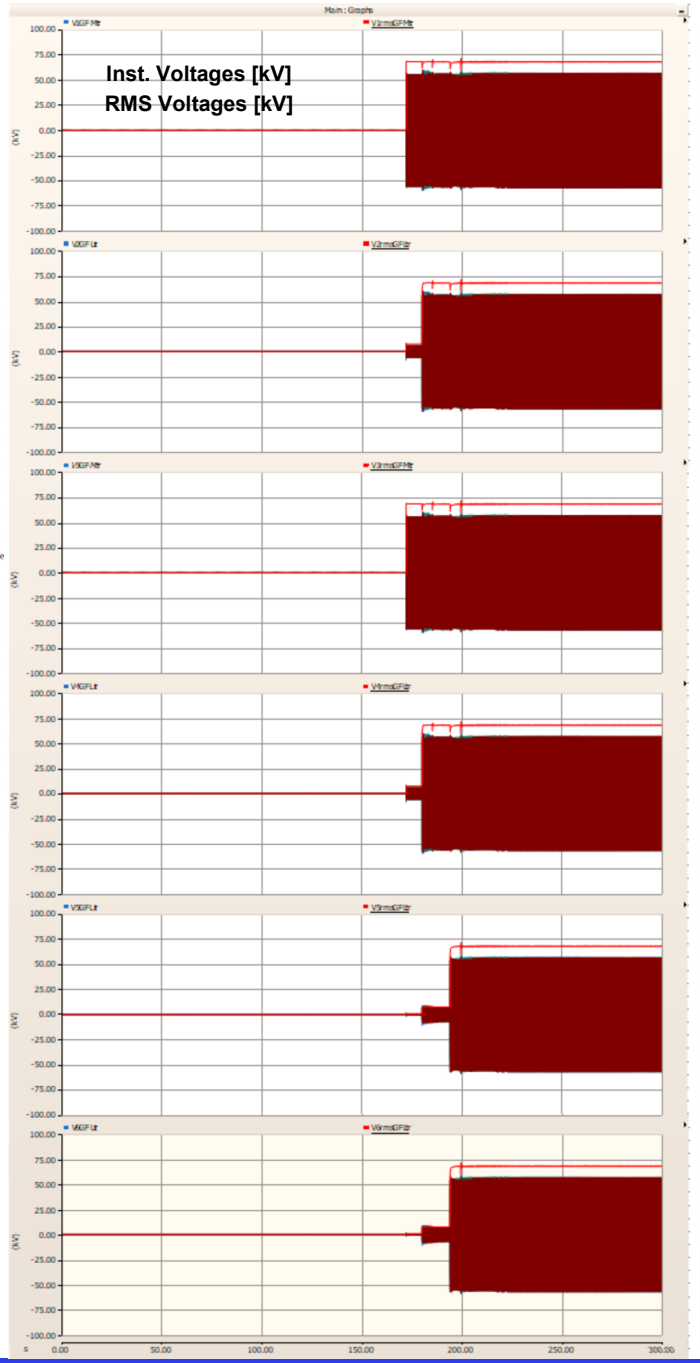
$$T_{\text{aero}} > 0 \implies \omega_{\text{r}} \uparrow \implies E_{\text{PMSG}} \uparrow \implies V_{\text{dc}} \uparrow \implies V_{\text{GSC}} \uparrow$$

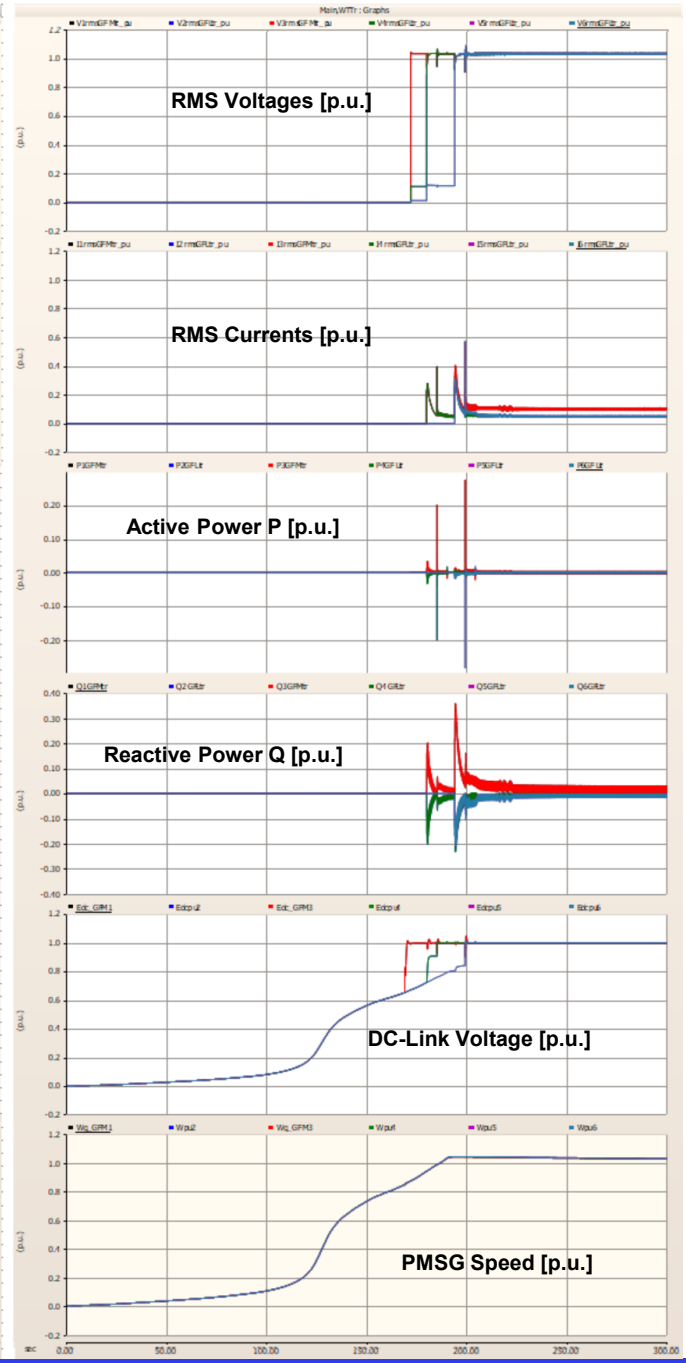
Two-string blackstart

Two-String Six-Turbine Model 4.5 m/s



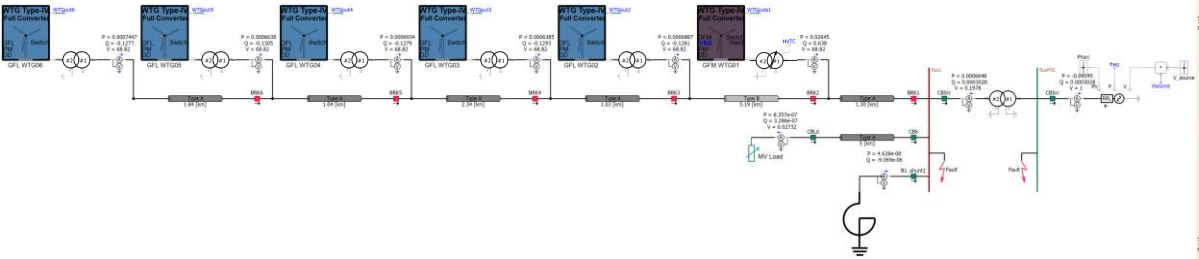
- Successful 6-WT no-load restoration, with stable operation through 300 s.
- Settled voltage ≈1.03 pu and peak converter current ≈0.59 pu meet the corresponding study limits.
- DC voltage settles near 1.00 pu; rotor speed peaks around 1.05 pu.
- Strings have the same cable types and distances. What happens if different (see slide 15)?
- Same DC voltage and ω speed because of identical wind inputs and initial conditions → different wind profiles wake effects necessary?



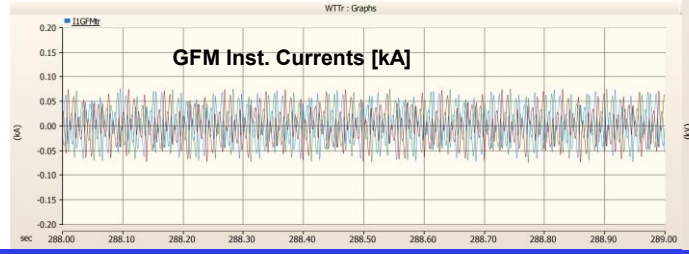


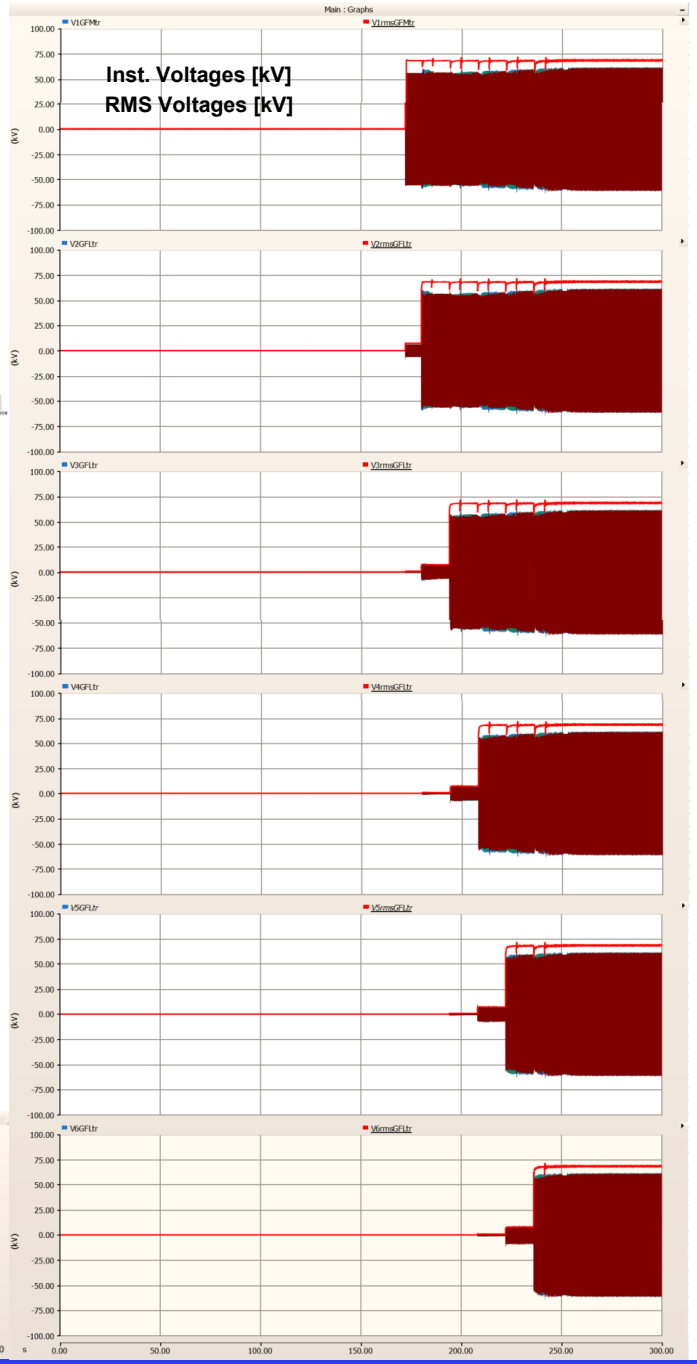
Single-string blackstart

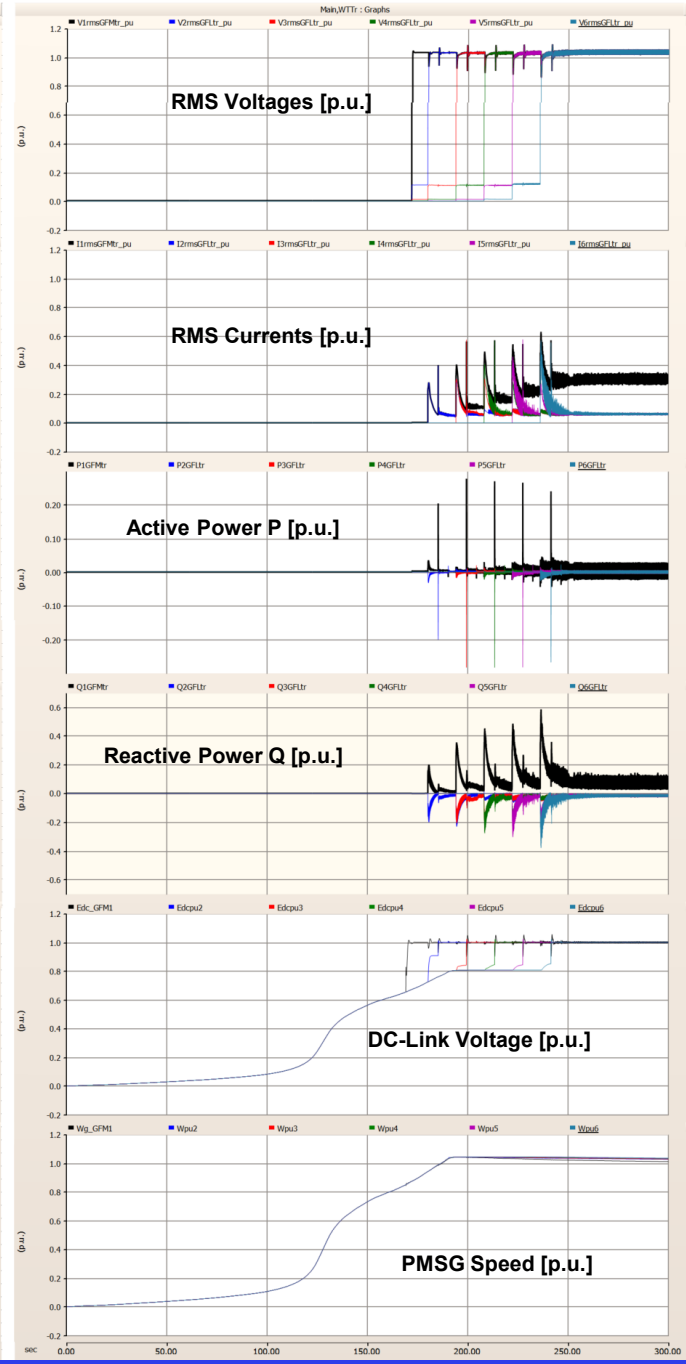
One-String Six-Turbine Model 4.5 m/s



- One GFM restores five GFL turbines at 4.5 m/s; operation remains bounded through 300 s.
- Collector voltage settles around 1.03–1.05 pu; DC voltage remains near 1.00 pu.
- Successive connections produce stronger P, Q and I disturbances than in the mirrored two-string case.
- The longer feeder places the full network-balancing burden on one GFM, increasing its current and connection disturbances.
- GFM current settles around 0.30 pu, with connection peaks approaching 0.6–0.65 pu; instantaneous current waveforms confirm persistent distortion.
- Results implicate feeder extension and reduced GFM support collectively; the dominant interaction remains to be identified.

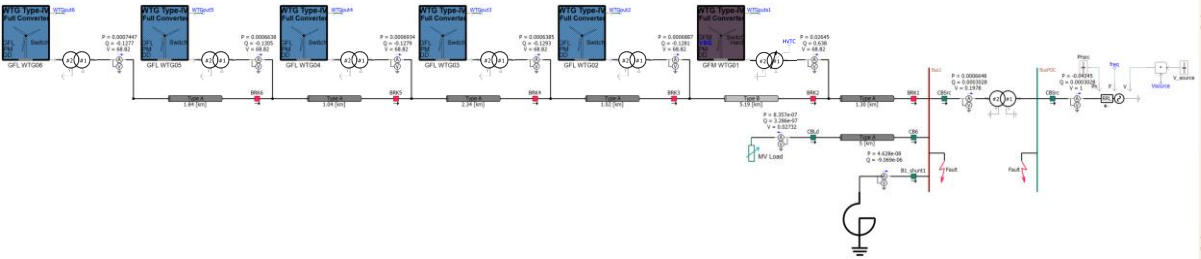




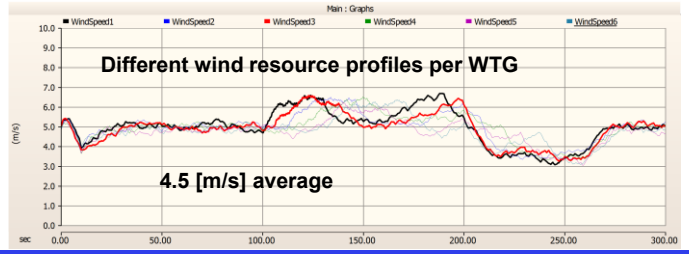


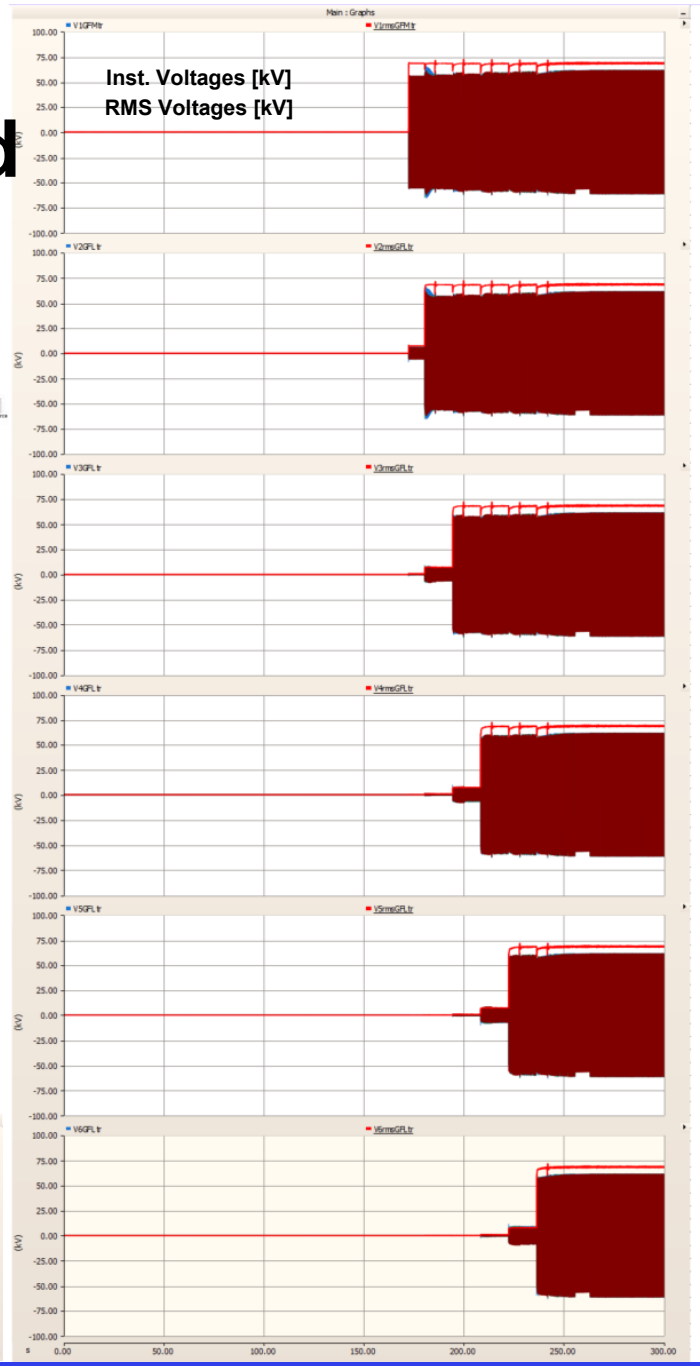
Single string, variable wind

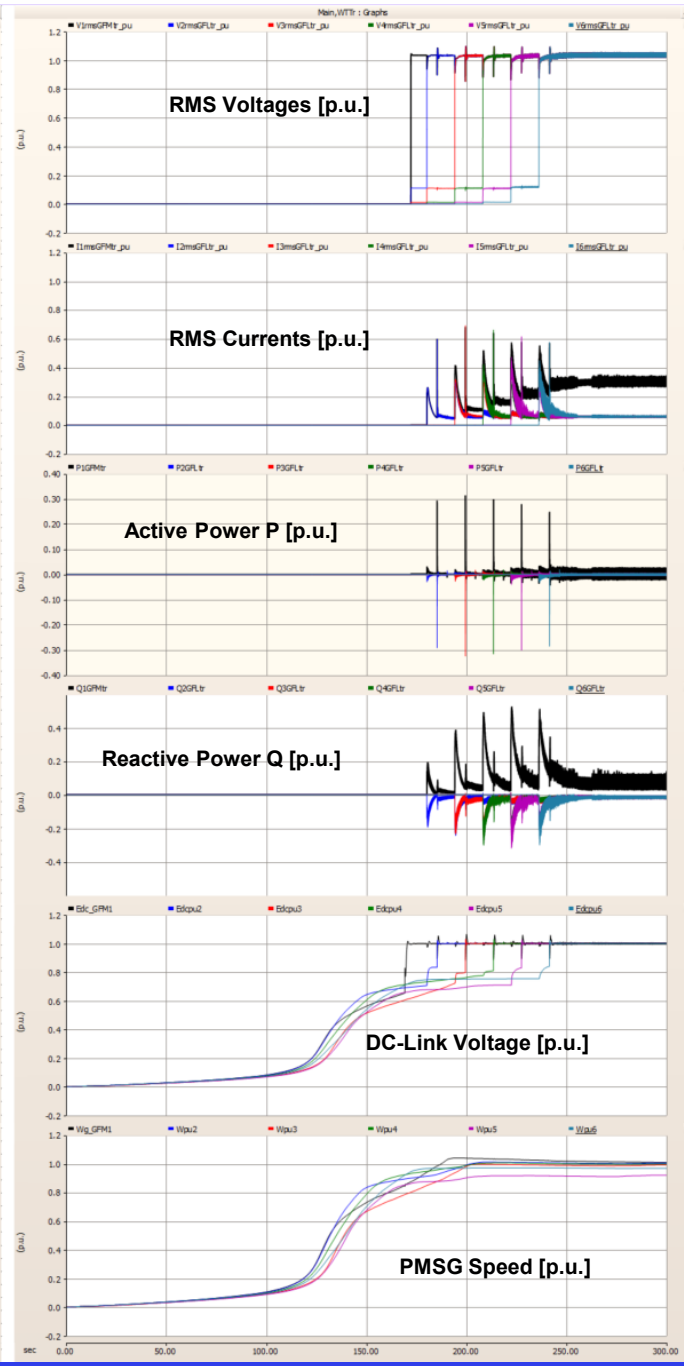
Individual wind profiles 4.5 m/s average



- Test with specific wind energy source profiles for each WTG.
- One GFM restores five GFL WTGs despite different wind profiles and startup readiness times.
- Collector voltage recovers to approximately 1.03–1.05 pu; DC-link voltages settle near 1.00 pu.
- Rotor-speed trajectories differ, while the electrical response remains bounded through 300 s.

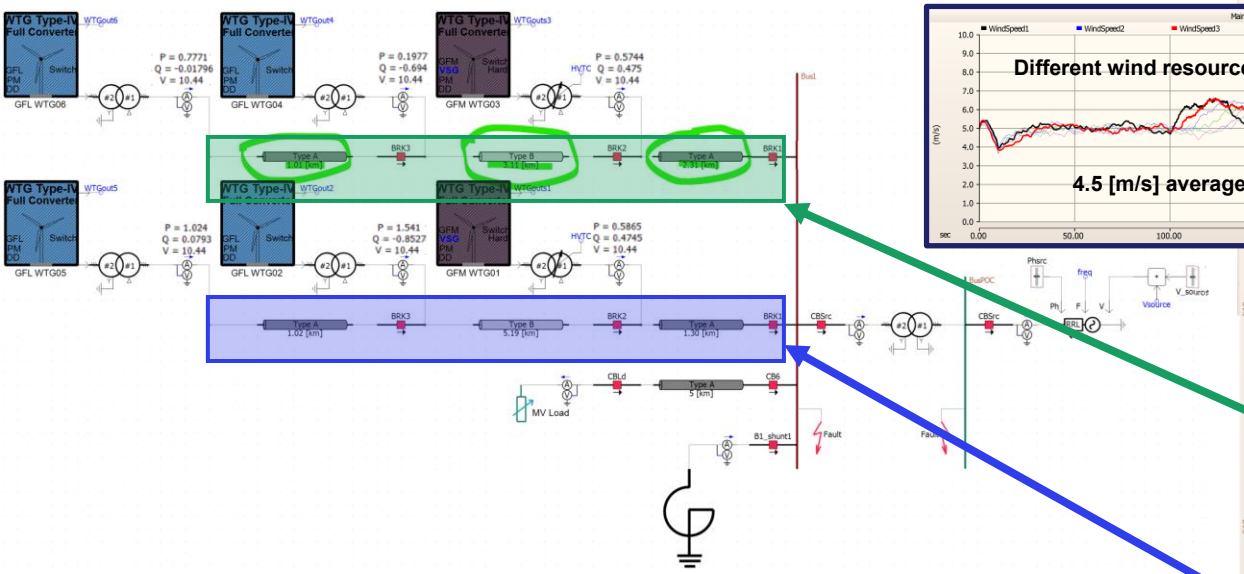


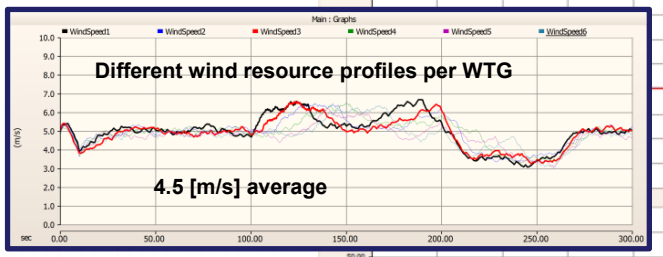


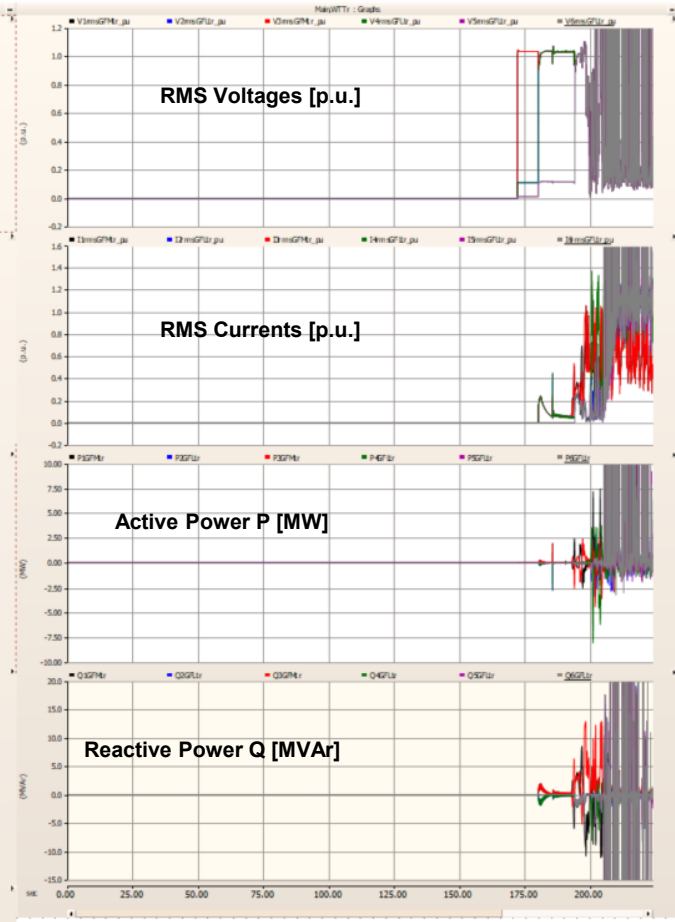


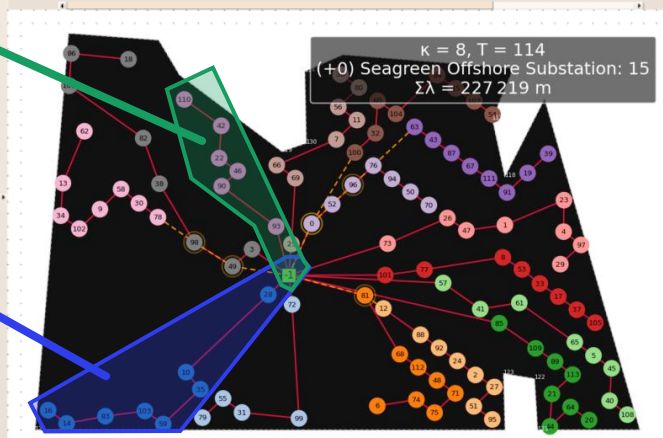
Unequal collector strings

Instability after GFL connection at 4.5 m/s









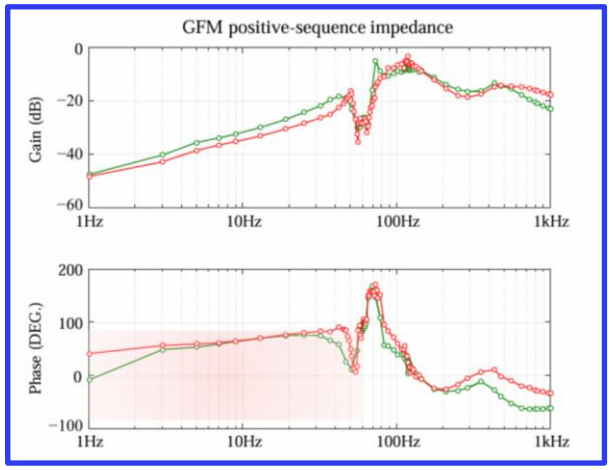
- Different cable types and lengths produce an unstable two-string response around 200 s, following the final two GFL startup events.
- P, Q and current oscillations grow; voltage regulation is lost and current exceeds 1.00 pu.
- The stable mirrored case does not demonstrate robustness to collector-network diversity.
- Cable length and type changed together; their individual contributions remain unresolved.
- Different wind profiles perceived in every WTG also resulted in unsuccessful restoration, with persistent undervoltage and elevated GFM currents.

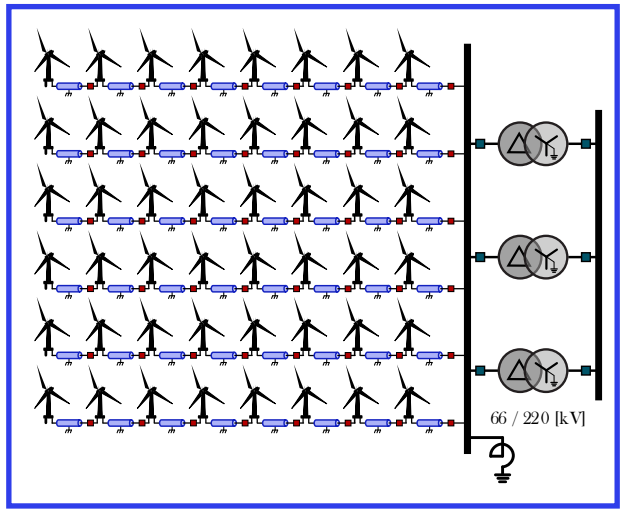
[15], [17]

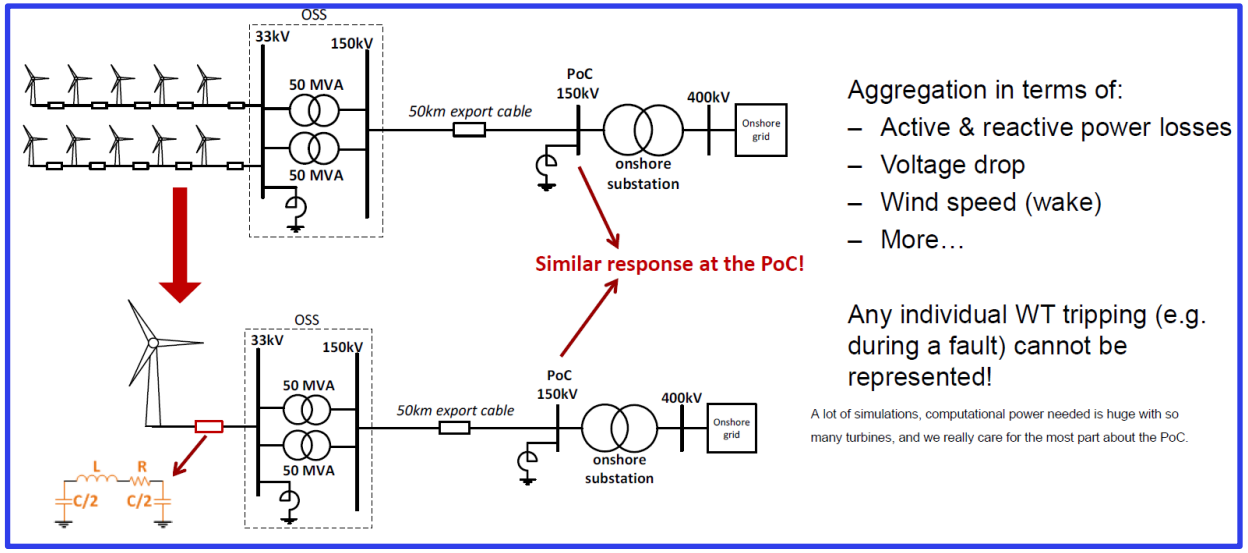
Next Steps

Validation, model reduction and extension to Stage 2

Target	Details	Why
Frequency-domain studies and restoration robustness	Use impedance-based analysis at settled operating points; test control adjustments and sequential string energisation in EMT with different conditions.	Identify the interactions behind poor voltage recovery and establish acceptable restoration across wind conditions and collector configurations.
Soft Energisation variant	Repeat the restoration sequence using controlled voltage build-up and compare it with R_V / POW Hard Energisation.	Determine whether Soft Energisation reduces switching stress while preserving stable restoration.
Final OWPP Representation	Compare a hybrid model with one or two explicit GFM turbines, one or two explicit GFL turbines, passive aux. equivalents against a fully aggregated model.	Find the lowest model complexity that still preserves blackstart dynamics of interest. Target is total cable / impedance? Full aggregation is enough. Target is WTGs Control interactions? Full aggregation not enough.
HV Export Transformer Energisation	Energise the offshore HV export transformers from the restored OWPP.	Demonstrate completion of the de-energised OWPP stage and assess inrush, voltage disturbance and converter loading.







[18], [19]

References

[1] F. Blaabjerg—"Reliability of IBR-dominated Power Systems", presented at the Imperial Summer School on IBR-dominated Power Systems, London, UK, Sep. 2024.
[2] L. Noris, O. Saborío-Romano, D. Müller, and B. Zoghdar, "Offshore Wind Blackstart & Restoration: State-of-the-Art Literature Review," 24th Wind & Solar Integration Workshop, Berlin, Germany, 7–10 Oct. 2025.
[3] PSCAD, "Type-4 Wind Turbine Model: For PSCAD Version v4.6 and better," Rev. 3, 3 Dec. 2018. Official documentation.
[4] M. Shan, W. Shan, F. Welck, and D. Duckwitz, "Design and laboratory test of black-start control mode for wind turbines," Wind Energy, vol. 23, no. 3, pp. 763–778, 2020, doi: 10.1002/we.2457.
[5] K. E. Johnson, L. Y. Pao, M. J. Balas, V. Kulkarni, and L. J. Fingersh, "Stability Analysis of an Adaptive Torque Controller for Variable Speed Wind Turbines," NREL/CP-500-36756, Dec. 2004, Eqs. (17)–(18). Report.
[6] P. Bortolotti, H. Canet Tarrés, K. Dykes, K. Merz, L. Sethuraman, D. Verelst, and F. Zahle, "IEA Wind TCP Task 37: Systems Engineering in Wind Energy—WP2.1 Reference Wind Turbines," NREL/TP-5000-73492, May 2019, doi: 10.2172/1529216.
[7] A. Avazov, "AC Connection of Wind Farms to Transmission System: from Grid-Following to Grid-Forming," doctoral thesis, Centrale Lille and KU Leuven, 2022, Fig. 1.27, p. 36.
[8] G. Huang, F. Shen, S. Huang, Q. Wu, J. Wei, Y. Qu, and P. Wang, "Novel Black Start Control Strategy With Power Boundary Analysis for PMSG-Based Wind Turbines," IEEE Transactions on Sustainable Energy, vol. 15, no. 2, pp. 1224–1238, Apr. 2024, doi: 10.1109/TSTE.2023.3332845.
[9] A. Jain, O. Saborío-Romano, J. N. Sakamuri, and N. A. Cutululis, "Virtual Resistance Control for Sequential Green-start of Offshore Wind Power Plants," IEEE Transactions on Sustainable Energy, vol. 13, no. 3, pp. 1420–1429, 2022, doi: 10.1109/TSTE.2022.3159620.
[10] National Grid ESO, "Black Start from Non-Traditional Generation Technologies: Technology Capability and Readiness for Distributed Restoration," Network Innovation Allowance (NIA), Report 1, prepared by TNEI Services Ltd., June 2019.
[11] CIGRE Working Group C2.26, Power system restoration accounting for a rapidly changing power system and generation mix, Technical Brochure 911, Aug. 2023.
[12] Enspec Power Ltd., "Case Study: Point-on-Wave Switching at Viking Wind Farm," technical case study.
[13] CIGRE UK, "Transformer energisation in power systems," Technical Insight 568, n.d. [Online].
[14] TotalEnergies, "Seagreen: Offshore wind farm turns wind into current," n.d. Accessed: Sep. 10, 2026. [Online].
[15] M. Souza de Alencar, T. Göçmen, and N. A. Cutululis, "Flexible cable routing framework for wind farm collection system optimization," European Journal of Operational Research, vol. 329, no. 3, pp. 1037–1051, 2026, doi: 10.1016/j.ejor.2025.07.069.
[16] Ö. Göksu, O. Saborío-Romano, N. A. Cutululis, and P. E. Sørensen, "Black Start and Island Operation Capabilities of Wind Power Plants," in Proceedings of the 16th Wind Integration Workshop, Berlin, Germany, Oct. 25–27, 2017.
[17] PROMOTioN, "Detailed functional requirements to WPPs," Deliverable 3.1, Version 1.0, 21 Dec. 2016.
[18] N. A. Cutululis, "M04 – Control and Dynamic Models of Wind Turbines," lecture slides, course 46550: Offshore Wind Grid Connection and HVDC Transmission, DTU Wind, Technical University of Denmark, Sept. 26, 2025.
[19] W. Yan, S. Shah, V. Gevorgian, P. Koralewicz, R. Wallen and D. W. Gao, "On the Low Risk of SSR in Type III Wind Turbines Operating With Grid-Forming Control," in IEEE Transactions on Sustainable Energy, vol. 15, no. 1, pp. 443-453, Jan. 2024.
[20] T. Green, "Power system stability with a high penetration of inverter-based resources", presented at the Imperial Summer School on IBR-dominated Power Systems, London, UK, Sep. 2024.
[21] B. Kroposki, "UNIFI Consortium for Grid Forming Inverters", presented at the IREDonline 2025 Resilience and Stability in Power Systems with Very High Shares of Renewable Energy Sources, online, Jun. 2025.
[22] B. Kroposki, B. Johnson, Y. Zhang, V. Gevorgian, P. Denholm, B. M. Hodge, and B. Hannegan, "Achieving a 100% Renewable Grid: Operating Electric Power Systems with Extremely High Levels of Variable Renewable Energy", IEEE Power and Energy Magazine, Vol. 15, Mar. 2017 [Online].
[23] IEEE Standards Association, IEEE Std 2800-2022, "IEEE Standard for Interconnection and Interoperability of Inverter-Based Resources Interconnecting with Associated Transmission Electric Power Systems", Piscataway, NJ, USA, Apr. 2022. [Online].
[24] P. Kundur, "Power System Stability and Control", New York, NY, USA: McGraw-Hill, 1994.
[25] A. Jain, "Green Black-Start of HVDC-Connected Offshore Wind Power Plants Using Grid-Forming Control", PhD Thesis Report, Technical University of Denmark, 2021.
[26] National Energy System Operator (NESO), "GC0137: Minimum Specification Required for Provision of GB Grid Forming (GBGF) Capability", 2024 [Online].
[27] D. Pagnani, "Design and Integration of Black-Start Service Provision by Offshore Wind Farms", PhD Thesis Report, Aalborg Universitet, 2023.
[28] Florian Dörfler, "Fundamentals for IBR Control", presented at the Imperial Summer School on IBR-dominated Power Systems, London, UK, Sep. 2024.
[29] R. Rosso, X. Wang, M. Liserre, X. Lu, and S. Engelken, "Grid-Forming Converters: Control Approaches, Grid-Synchronization, and Future Trends—A Review", IEEE Open Journal of Industry Applications, vol. 2, pp. 93–109, Apr. 2021, doi: 10.1109/OJIA.2021.3074028.
[30] PROMOTioN, "Overview of the conducted tests, the results and the associated analyses with respect to the research questions and analyses within WP3," Deliverable D16.3, ver. 1.0, Feb. 27, 2020.
[31] Z. Zhang and X. Zhao, "Startup control of grid-forming offshore wind turbines connected to the diode-rectifier-based HVDC link," IEEE Transactions on Sustainable Energy, vol. 16, no. 1, pp. 407–418, 2025, doi: 10.1109/TSTE.2024.3454797.
[32] Energinet, "Immittance Measurement ToolBox (IMTB)," GitHub repository. [Online]. Available: github.com/Energinet-SimTools/IMTB. Accessed: Sep. 21, 2026.
[33] A. Hadjileonidas, Y. Zhu, D. Brahma, and T. C. Green, "Assessing Small-Signal System Strength Across Modes, Locations and Operating Conditions for Inverter Based Resource Connections," TechRxiv, preprint, Mar. 5, 2026. doi: 10.36227/techrxiv.177274582.25115226/v1.


DTU

Blackstart and system restoration

From an initial electrical island to system network recovery

- **Blackstart**—Initial process in which one and/or more generating units re-start and re-energise a small electric island; completed once that island can export power beyond its own auxiliaries.
- **System Restoration**—Follows Blackstart: Energising transformers, transmission lines and distribution feeders; synchronising islands; progressively re-connecting customer loads until the entire grid returns to normal operation.







[11]

Challenges for IBR Blackstart

Current limits, control interactions and coordinated startup

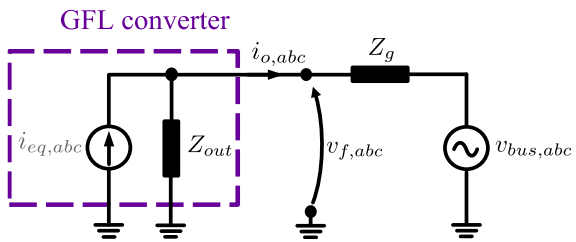
- Fast converter dynamics and limited overcurrent capability complicate energisation and protection.
- Lower short-duration overcurrent capability than synchronous generators.
- Much less unit capacity (compared to SGs).
- Fault-current magnitude and sequence content depend on converter controls.
- Protection settings must suit the changing restoration network.
- Many converter units require coordinated startup and stable power sharing.
- At least a handful of units need to be capable of self-starting, self-sustaining and energising other units without these capabilities.
- IBR Blackstart → a GFM Service

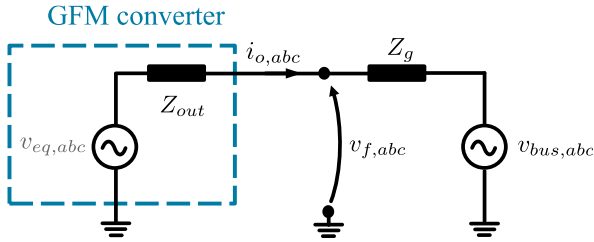
Generator Technology comparison for blackstart			
Technology	Heavy Synchronous	Inverter (Solar)	PMSG + Converters (Wind)
Unit Capacity [MVA]	~650–1900	~9	~20
Unit Physical Inertia [GWs]	~2.5	0	~0.2
Fault Current [p.u.]	~5–9	~1.2–2	
Virtual Inertia [GWs]	0	~0.5–3	
Grid Inertial response	Natural rotor response	Control and energy/headroom dependent	
# Unit/Modules	~3–6	~110	~50–70
Control timescales	Dynamics well separated–fast electrical and slow mechanical	Fast inner loops with slower outer and energy controls–overlapping and interacting dynamics	
Dynamic interactions	Machine, controls and network	Converter and network	Converter, network and rotor
Blackstart Readiness	Mature	Early Research	Demo Projects

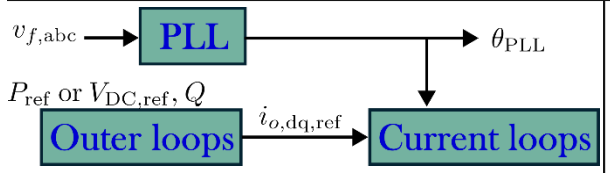
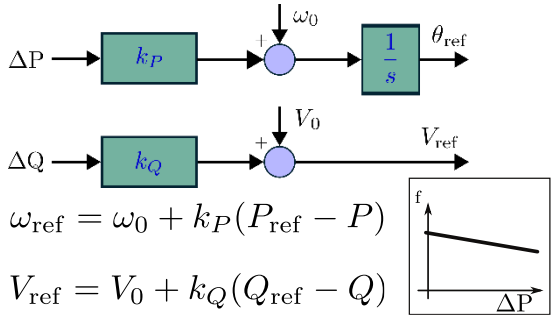
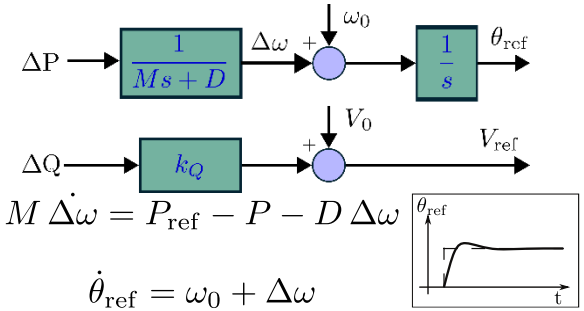
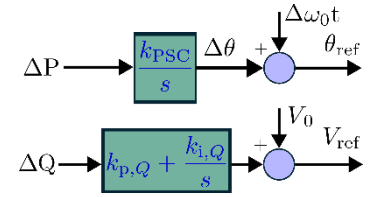
[11], [20], [21], [22], [23], [24]

Converter Control Comparison

GFL vs GFM (Droop / VSM / PSC)





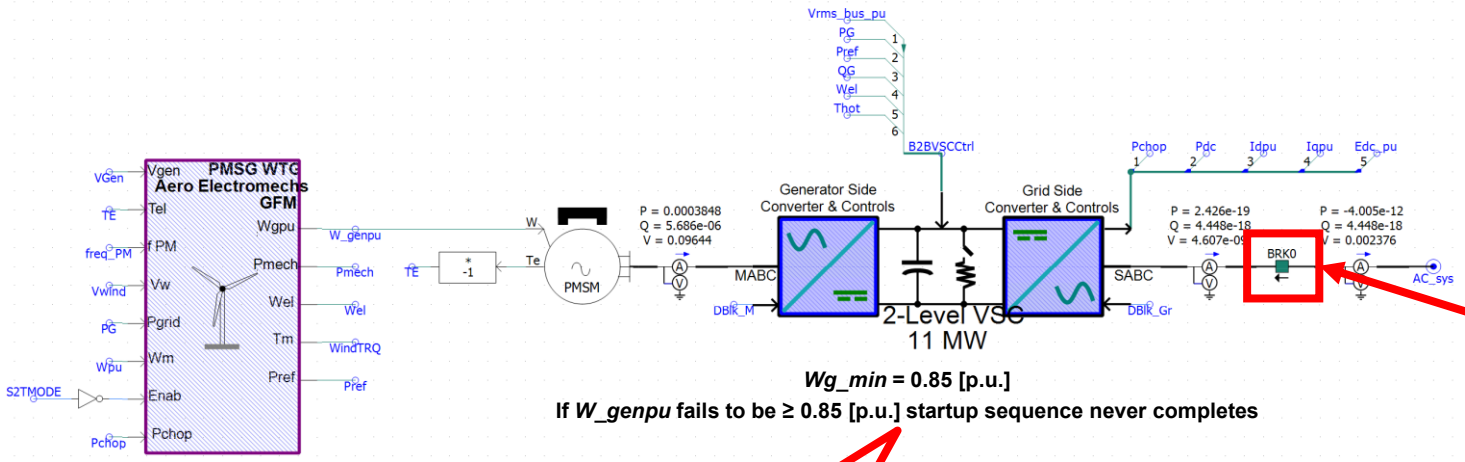
GFL	GFM Droop	GFM VSM	GFM PSC
PLL-based current control	Power–frequency / voltage slopes	Virtual synchronous machine	Power synchronisation control
 $\theta_{\mathrm{ref}} = \theta_{\mathrm{PLL}}$ $P \simeq \frac{3}{2} v_d i_d, \qquad Q \simeq -\frac{3}{2} v_d i_q$	 $\omega_{\mathrm{ref}} = \omega_0 + k_P(P_{\mathrm{ref}} - P)$ $V_{\mathrm{ref}} = V_0 + k_Q(Q_{\mathrm{ref}} - Q)$	 $M\,\dot{\Delta\omega} = P_{\mathrm{ref}} - P - D\,\Delta\omega$ $\dot{\theta}_{\mathrm{ref}} = \omega_0 + \Delta\omega$	 $\dot{\theta}_{\mathrm{ref}} = \omega_0 + k_{\mathrm{PSC}}(P_{\mathrm{ref}} - P)$ $\Delta P = P_{\mathrm{ref}} - P$
Mechanism PLL follows the island voltage. Outer loops set current references; inner loops track them.	**Mechanism** Power errors adjust frequency and voltage. Local droop slopes set load sharing.	**Mechanism** Power imbalance changes a virtual rotor speed; integrating speed gives the voltage angle.	**Mechanism** Power error directly advances or retards the voltage angle; voltage is controlled separately.
Advantages Direct power/current tracking. Straightforward current limiting.	**Advantages** Simple local power sharing. Few control parameters.	**Advantages** Tunable inertia and damping. Shapes frequency transients.	**Advantages** Simple angle synchronisation. No virtual rotor state to tune.
Limitations Cannot form a dead-bus voltage. PLL interactions can weaken stability in a small island.	**Limitations** Load-dependent V/f deviation. Network coupling and filtering affect sharing and stability.	**Limitations** Needs real energy/headroom. Poor inertia/damping tuning can cause oscillations.	**Limitations** Needs separate damping and current-limit design. Basic PSC has no explicit inertia setting.

[25], [26], [27], [28], [29]

Low-wind startup test < 4.5 m/s

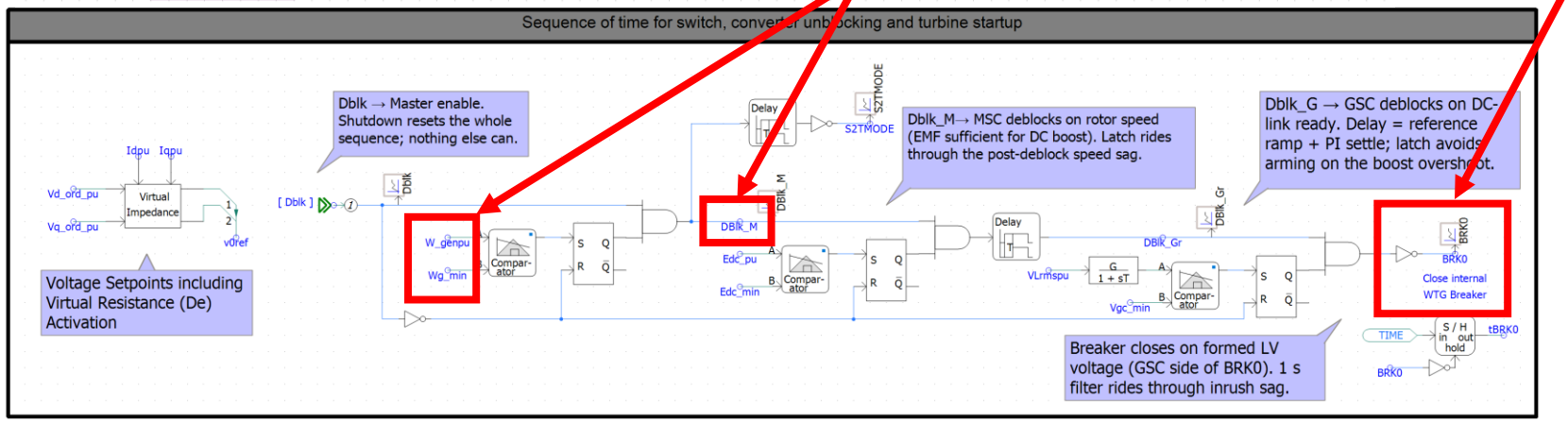
Startup interlock not reached in the reported 4 m/s run

- Preliminary test: A test was made with a wind input of 4 m/s but the result was not documented.
- GFM Startup sequence: Generator speed reportedly remained below the 0.85 pu startup threshold.
- The unmet speed condition blocked the subsequent converter startup sequence.
- Internal breaker *BRK0* and the external 66 kV breaker remained open; the collector stayed de-energised through 300 s.
- **Conclusion: Cut-in Wind Speed: 4 m/s → winds lower than 4.5 m/s fail to provide sufficient torque for the anchor GFM units.**

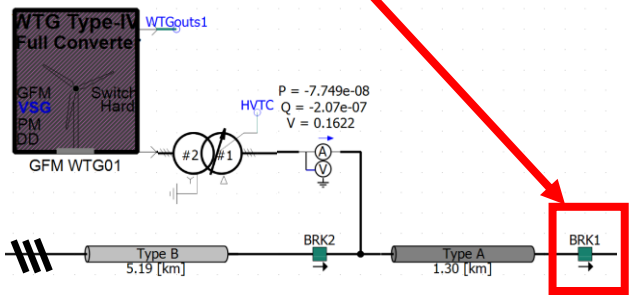


***Wg_min* = 0.85 [p.u.]**

If *W_genpu* fails to be ≥ 0.85 [p.u.] startup sequence never completes



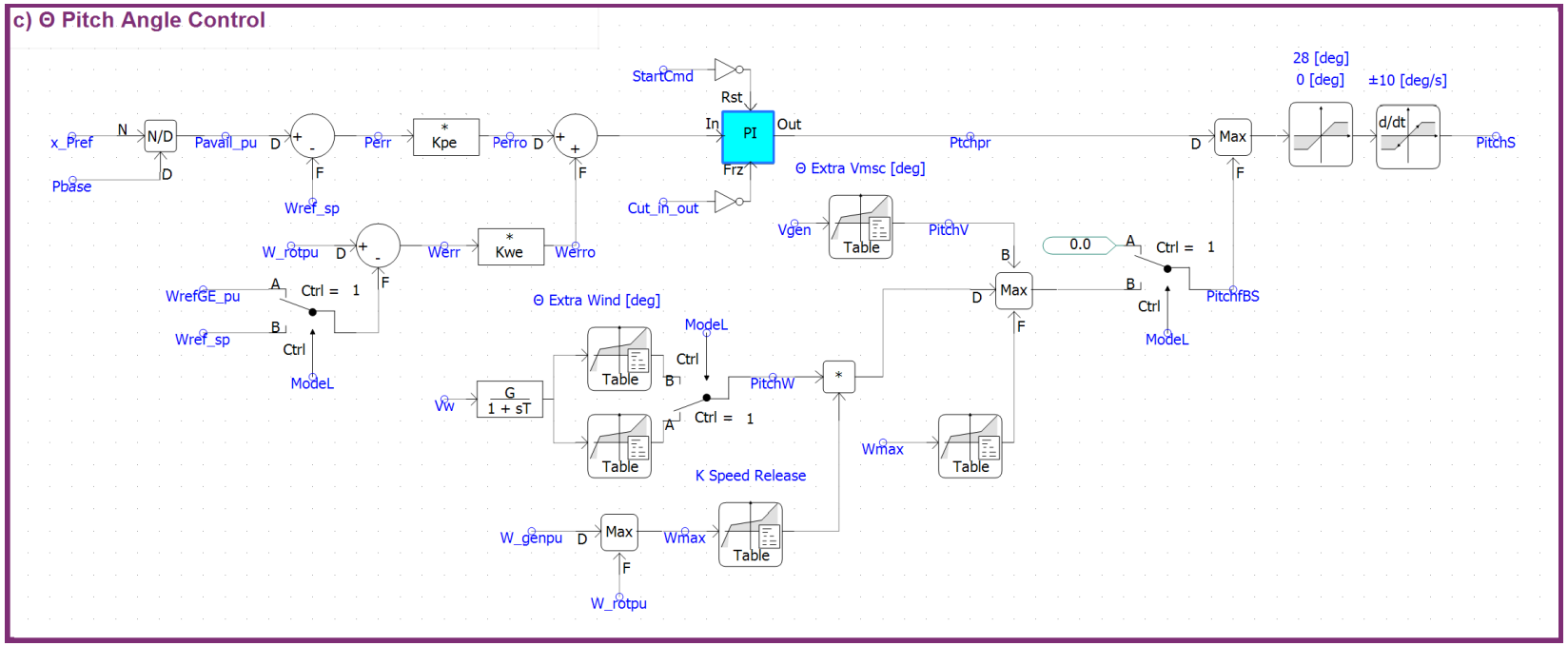
When Internal Breaker *BRK0* closes → external *BRK1* closes



Enhanced pitch control

Minimum-pitch supervision for low-load blackstart

Control structure



Why it was needed

- Low island demand can cause imbalance with excessive aerodynamic torque (abundant wind source).
- This can cause rotor acceleration which can raise machine-side voltage before the normal PI responds.

Functioning

- Speed release reduces the wind pitch floor when speed is low.
- The voltage floor stays active independently of speed release.
- MAX selects the largest request.

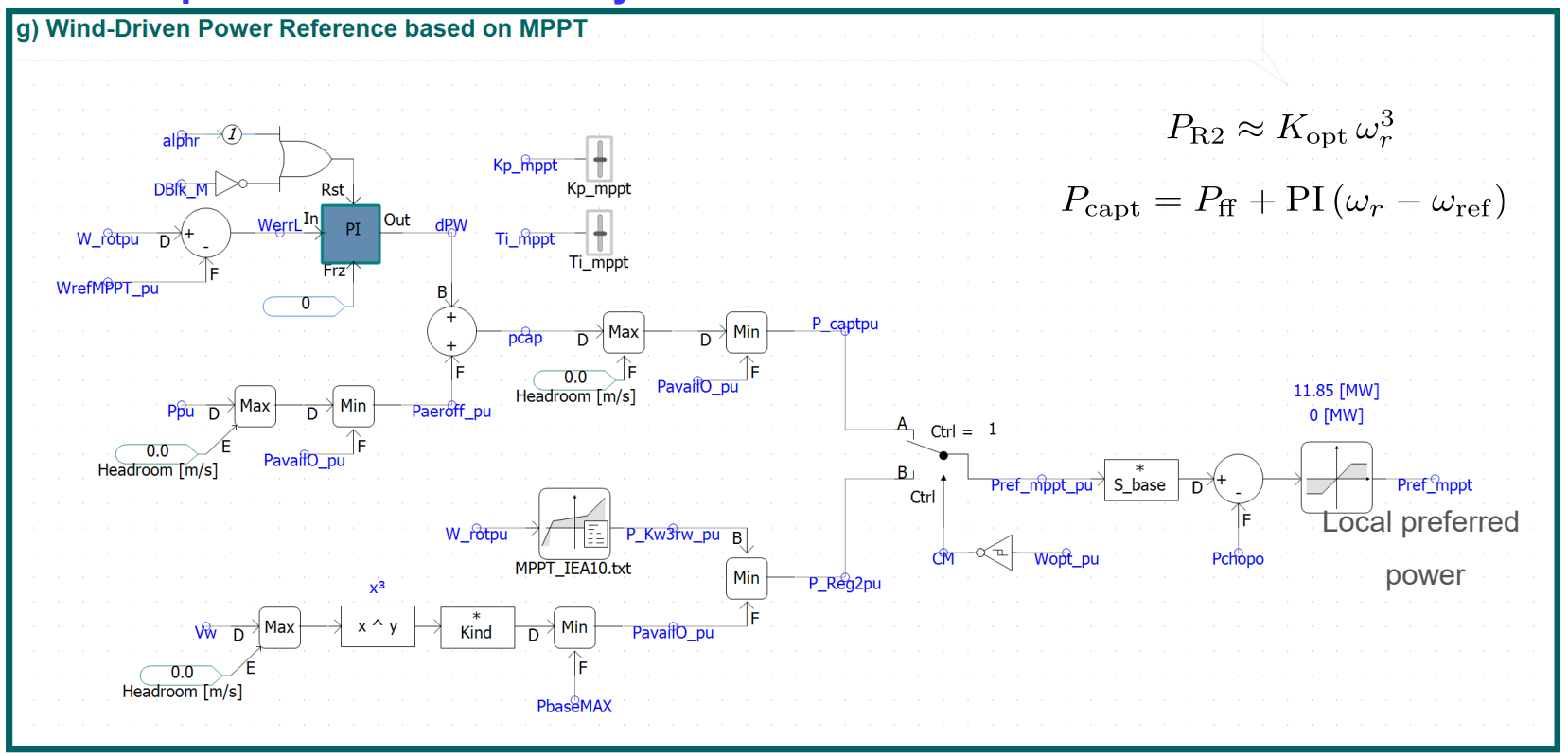
Used with soft and hard energisation. Pitch manages rotor energy and voltage stress on a slower timescale than inrush.

[4], [8]

Extended MPPT control

Wind-limited power references and minimum-speed operation

Local power-reference subsystem



$$P_{\mathrm{R2}} \approx K_{\mathrm{opt}}\,\omega_r^3$$

$$P_{\mathrm{capt}} = P_{\mathrm{ff}} + \mathrm{PI}\left(\omega_r - \omega_{\mathrm{ref}}\right)$$

Why it was needed

- The speed-only lookup could request near-rated power
- High rotor speed does not imply high sustainable wind power, especially during startup—WTG far from optimum operating point.

Functioning

- The speed PI reduces extraction when the rotor falls below target.
- The wind ceiling bounds either selected power branch.
- Actual aerodynamic power also depends on speed and pitch.

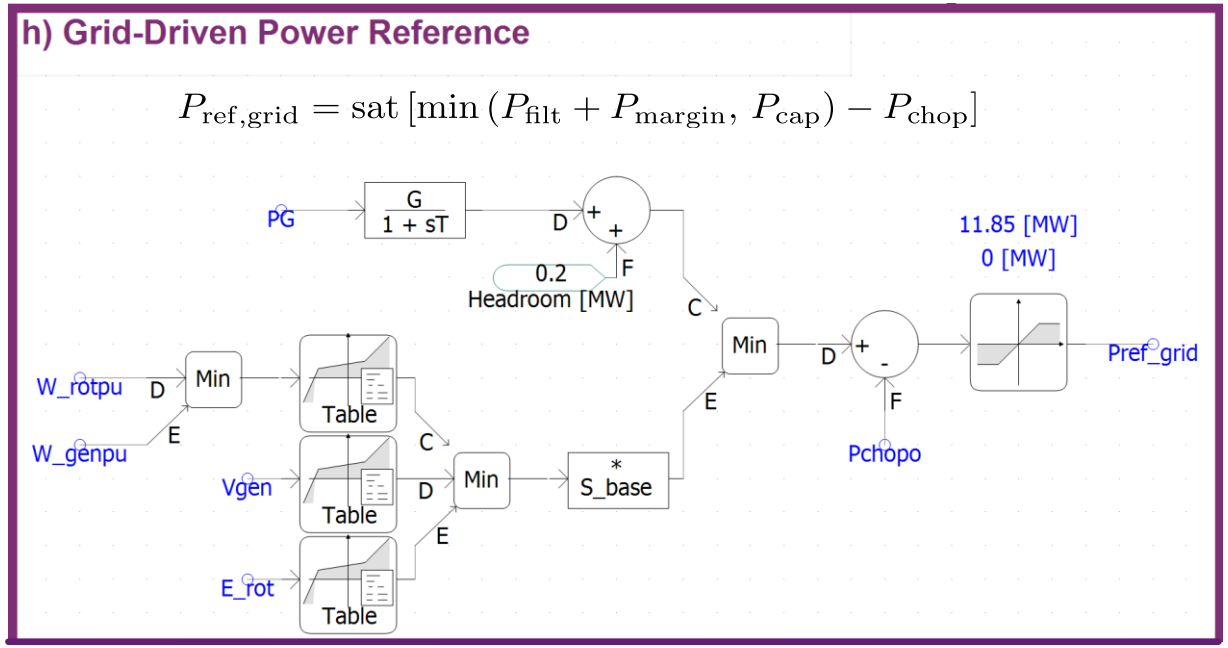
GFM power remains demand-driven. GFL references pass through startup and plant-dispatch supervision.

[6]

Grid-driven power-reference selection

GFM demand following with turbine capability limits

Grid-driven reference



Output passes through export-mode selection and reference ramp.

Why grid-driven

- During blackstart, a grid-driven Pref matches island demand within turbine limits, while MPPT or Cp-based references follow wind availability—may request more power than the island can absorb.
- Island demand sets GFM export, so, speed and pitch adapt wind capture to that demand.
- Rotor energy supplies the initial power mismatch.

Functioning

- Filter export and add a small power margin.
- Limited by operating limits, then subtract chopper power.
- This local Pref is only available in GFM WTGs.

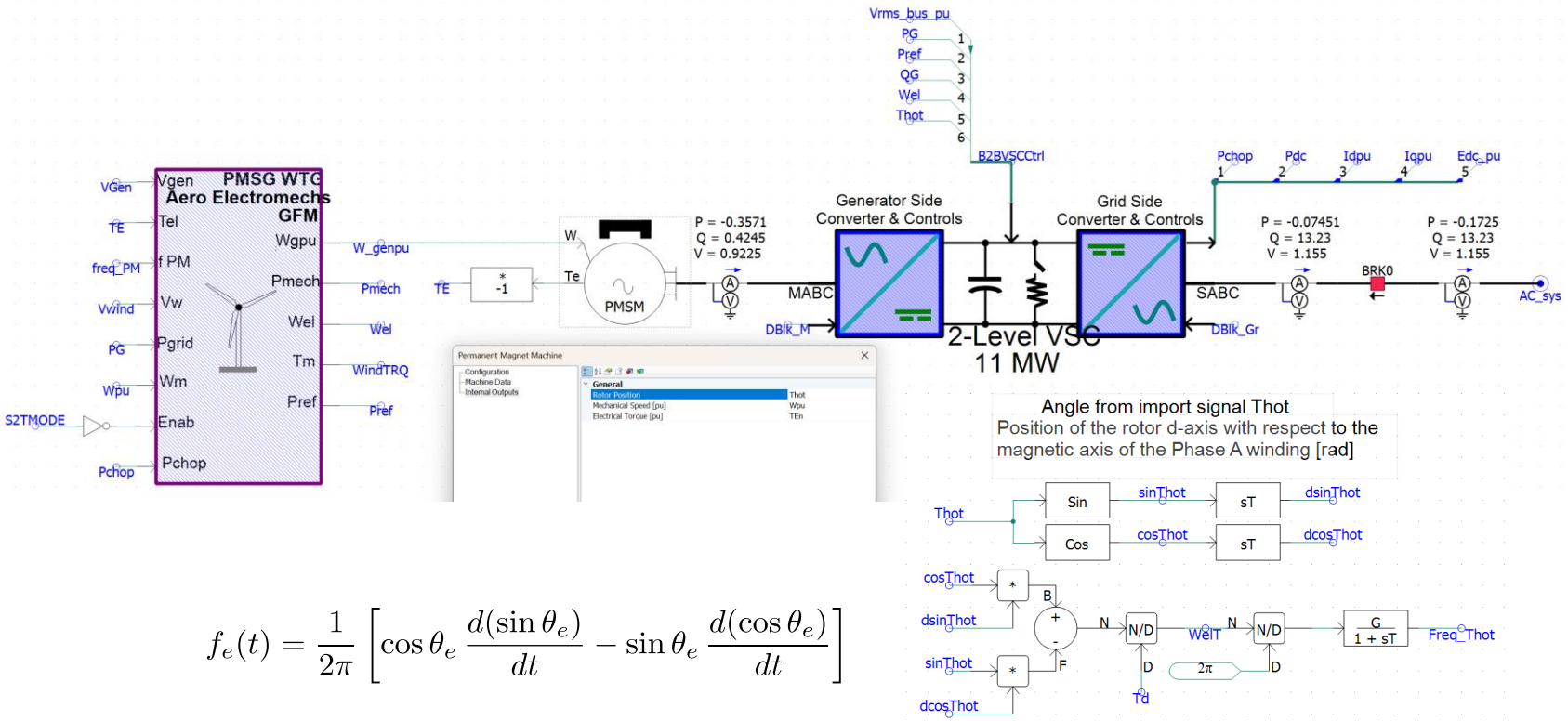
GSC forms voltage and frequency. MSC holds DC voltage. Pitch restores the mechanical–electrical power balance.

Local reference selection and WPP dispatch are separate. GFL followers use startup and plant-dispatched references.

[4], [8]

Voltage formation at the machine side converter MSC

Angle obtention from PMSG



$$f_e(t) = \frac{1}{2\pi}\left[\cos\theta_e \frac{d(\sin\theta_e)}{dt} - \sin\theta_e \frac{d(\cos\theta_e)}{dt}\right]$$

MSC Voltage formation

- Wind accelerates the permanent-magnet rotor, inducing AC voltage in the stator windings.
- The induced voltage magnitude and electrical frequency increase with rotor speed.
- Permanent magnets provide excitation; an external AC network is not required to generate this voltage.

Rotor angle and MSC control

- The PMSG output signal provides the rotor electrical angle for the MSC's *dq* transformations.
- The MSC uses this angle to control generator currents. In the GFM anchor, its outer control loop regulates DC-link voltage.
- Direct rotor-position information provides the control reference without a voltage PLL.

The sin/cos derivative of the rotor position calculates electrical speed while avoiding jumps caused by angle wrapping.

The PMSG supplies electrical energy. The MSC controls generator current and DC-link voltage. The GSC establishes collector voltage and frequency.

[3]

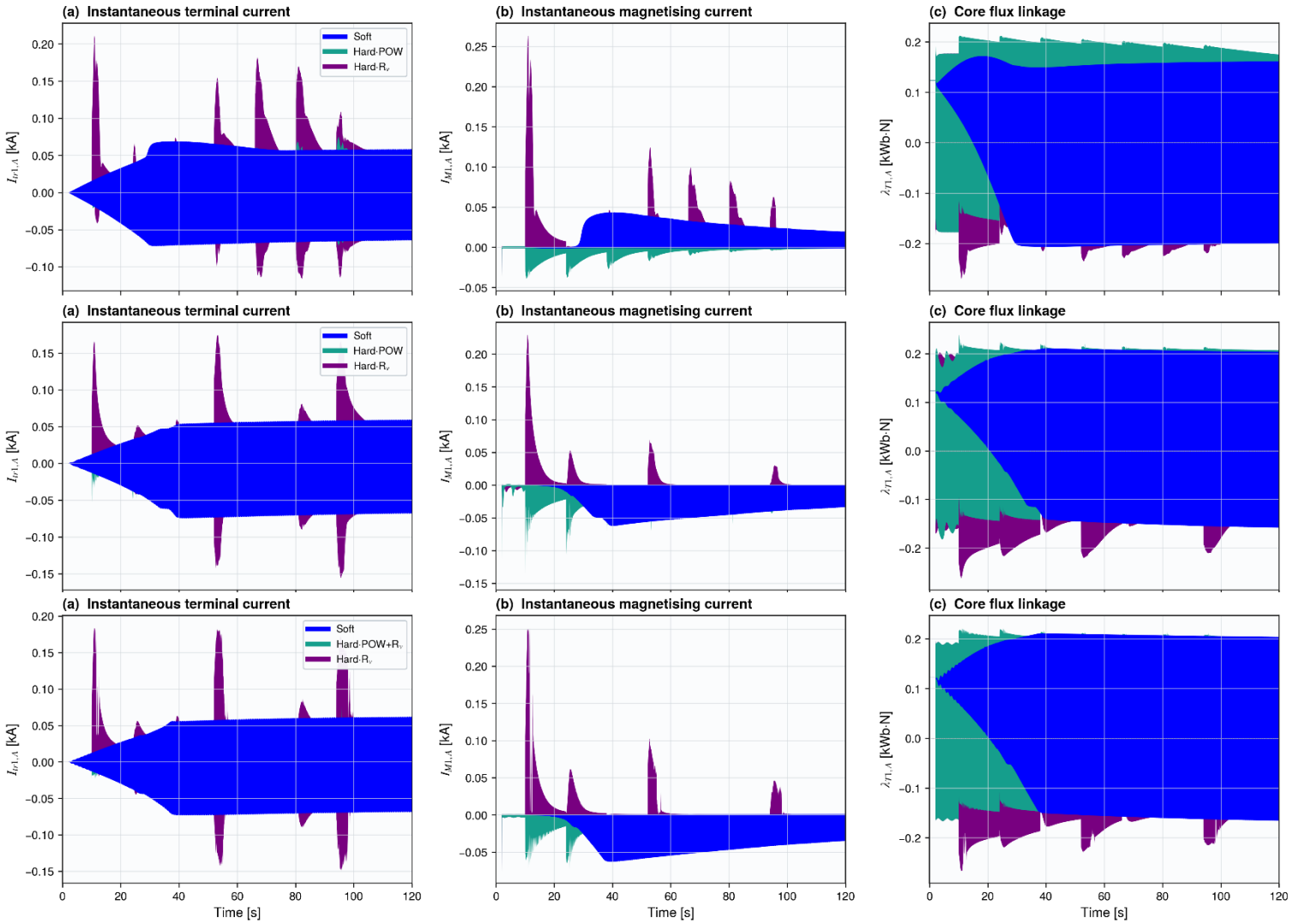
Transformer energisation at 8 m/s—Passive Loads

Magnetising current and core flux across the GFM controls

Droop

VSG / VSM

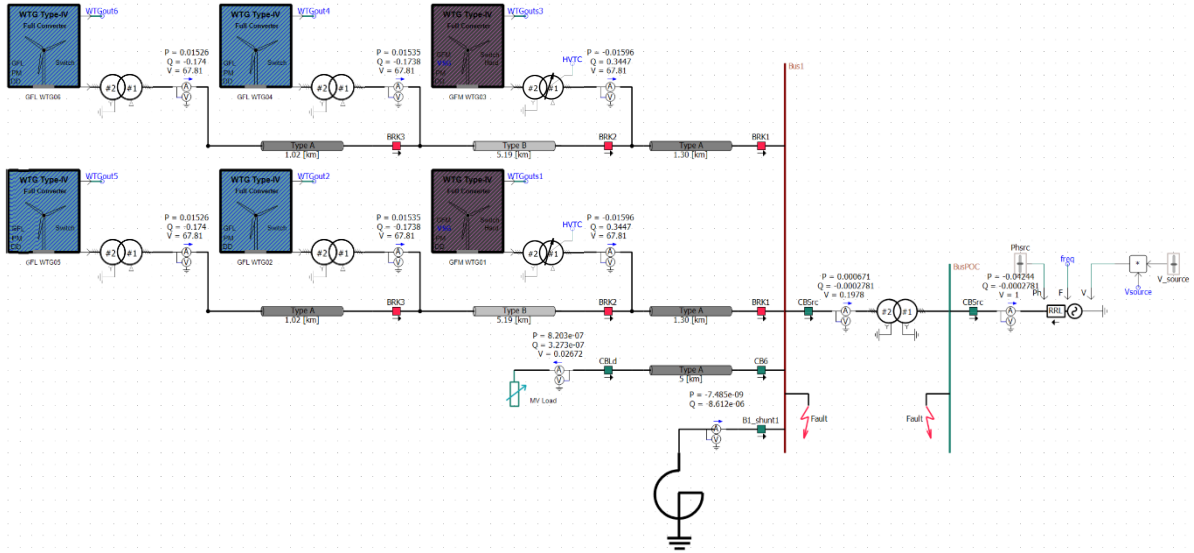
PSC



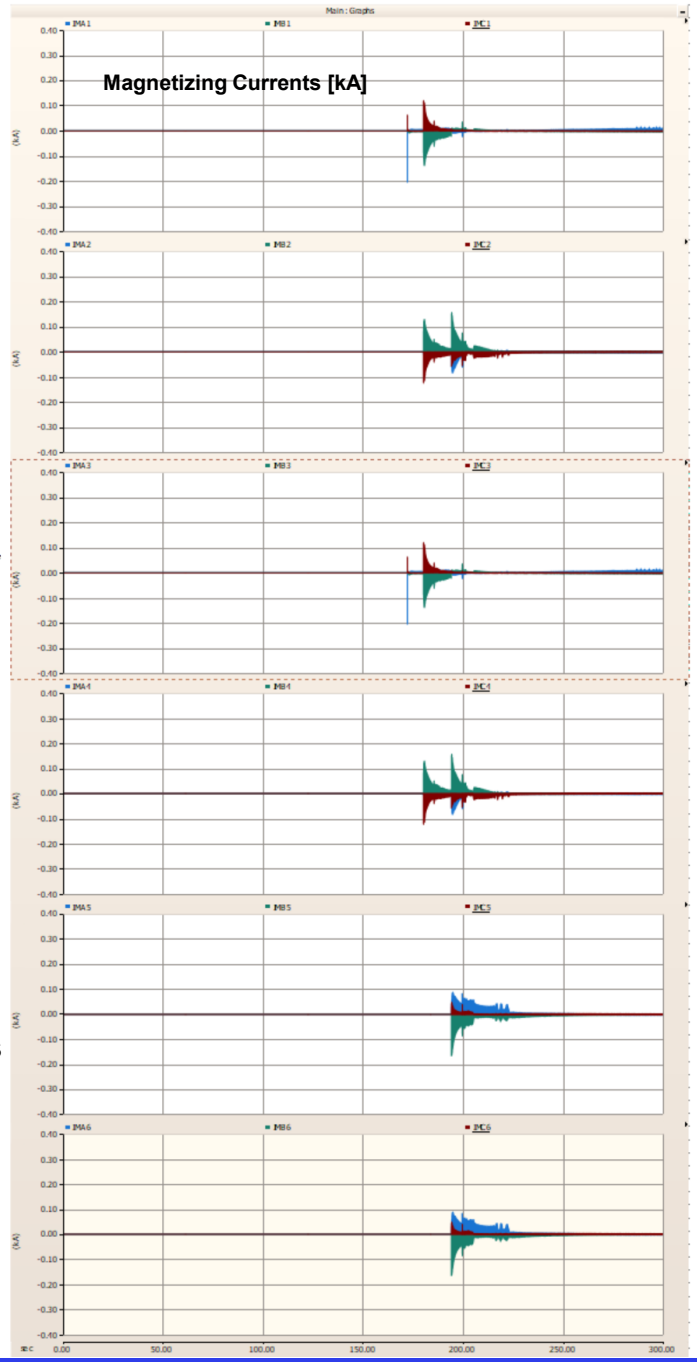
- Only phase A shown for clarity
- Phases B and C exhibit the same transient behaviour, offset by 120°

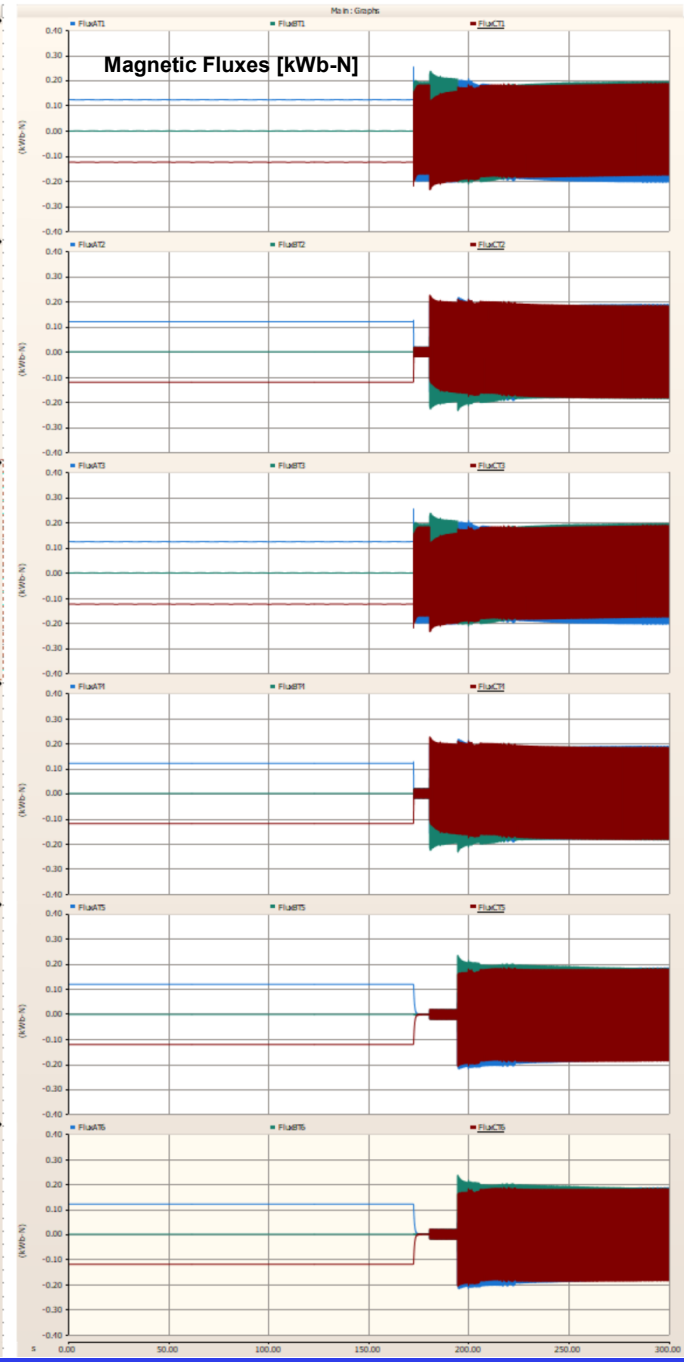
Transformer Energisation

Two-string case at 4.5 m/s



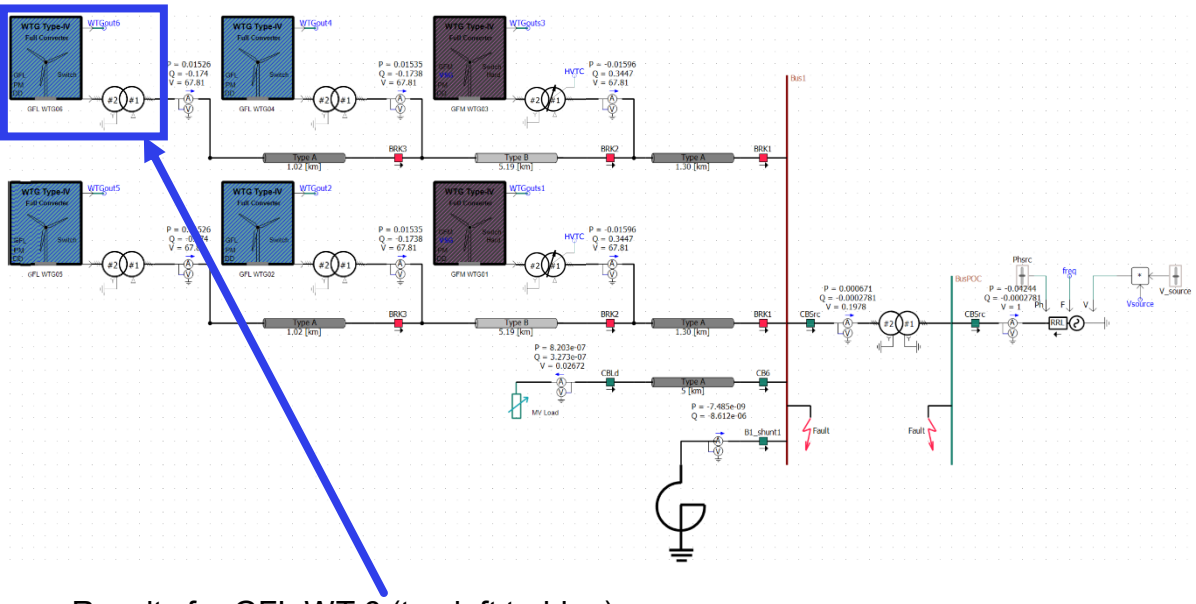
- Transformer magnetizing-current transients decay following successive connections.
- Magnetic flux remains bounded, supporting stable collector energisation through 300 s.
- Similar responses between corresponding turbines reflect matching parameters and simultaneous switching.



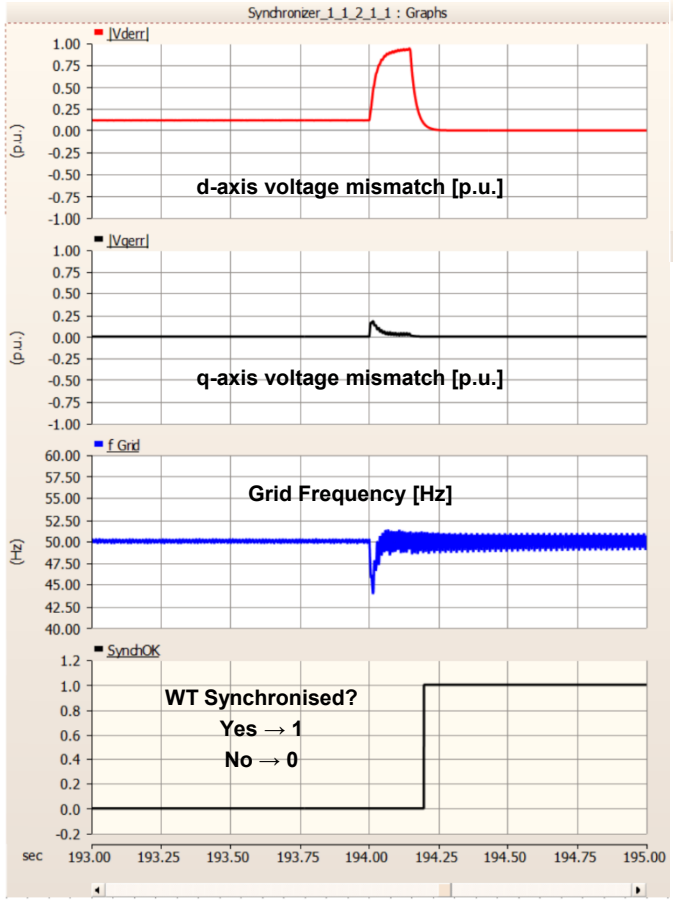


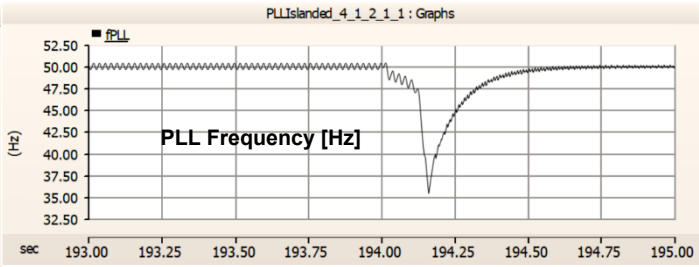
GFL WTGs Synchronisation

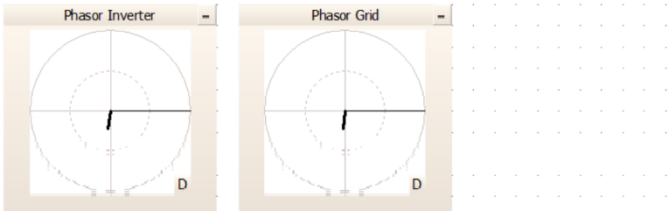
Two-string case at 4.5 m/s



- Results for GFL WT 6 (top left turbine)
- Synchroniser voltage errors decay; *SynchOK* asserts around 194.20 s.
- The local PLL returns to 50 Hz at approx. 194.8 s following voltage establishment.
- Successful connection is demonstrated; full synchronisation verification still requires phase-error limits and deblocking timing.
- GFL5 (bottom left turbine) exhibits the same behaviour as GFL6.

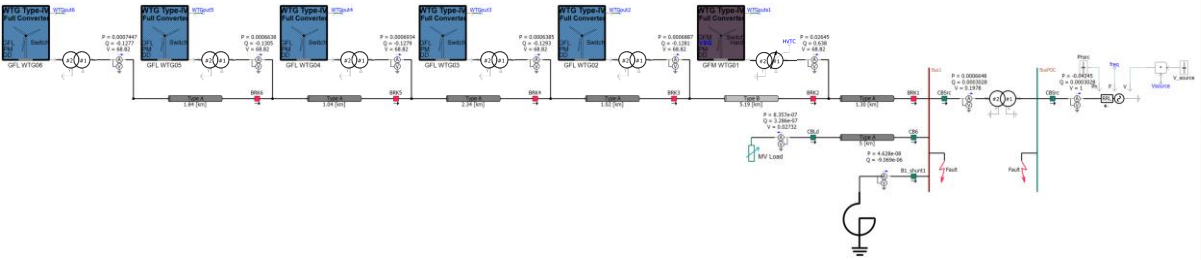




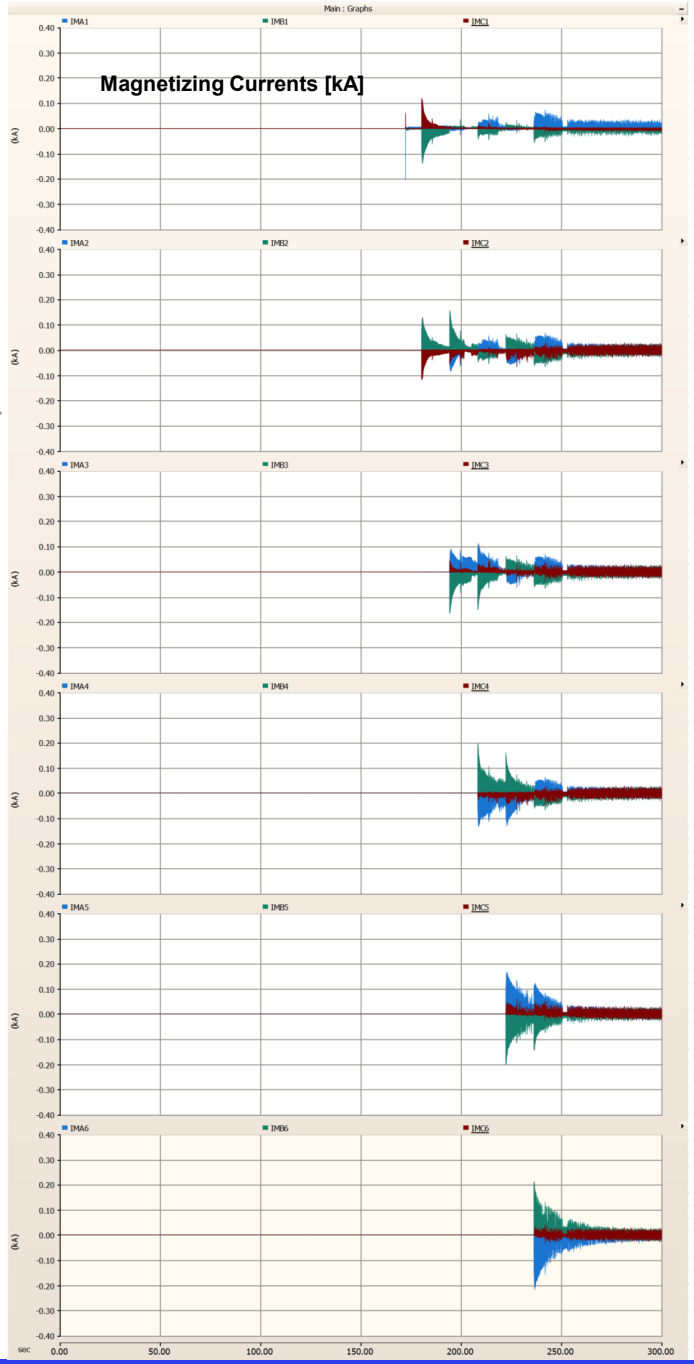


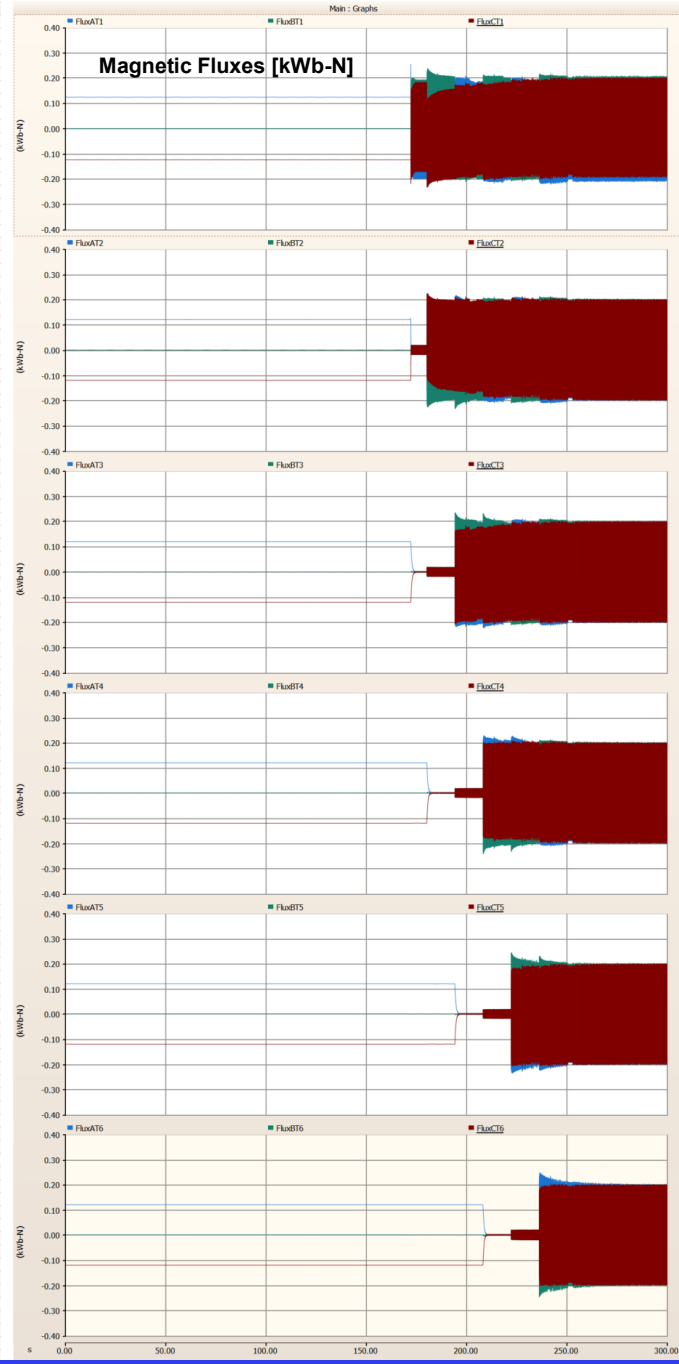
Transformer energisation

Results—One-String Six-Turbine Model



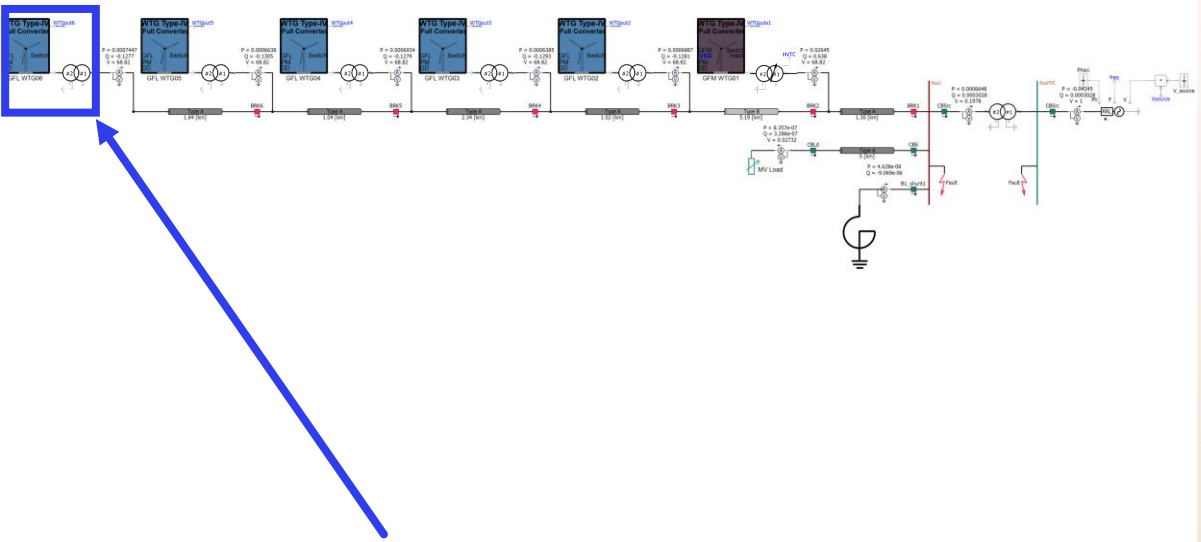
- Each new connection also disturbs transformers that are already energised.
- Main magnetising-current transients diminish; residual ripple exceeds the mirrored two-string case.
- The final transformer exhibits a magnetising-current transient of approximately 0.20 kA.
- Magnetic flux remains bounded through 300 s, without progressive drift.
- Compared to the two-string case (fewer WTGs per string) magnetizing currents show more ripple.
- Saturation and hysteresis settings still require verification against the transformer characteristics.

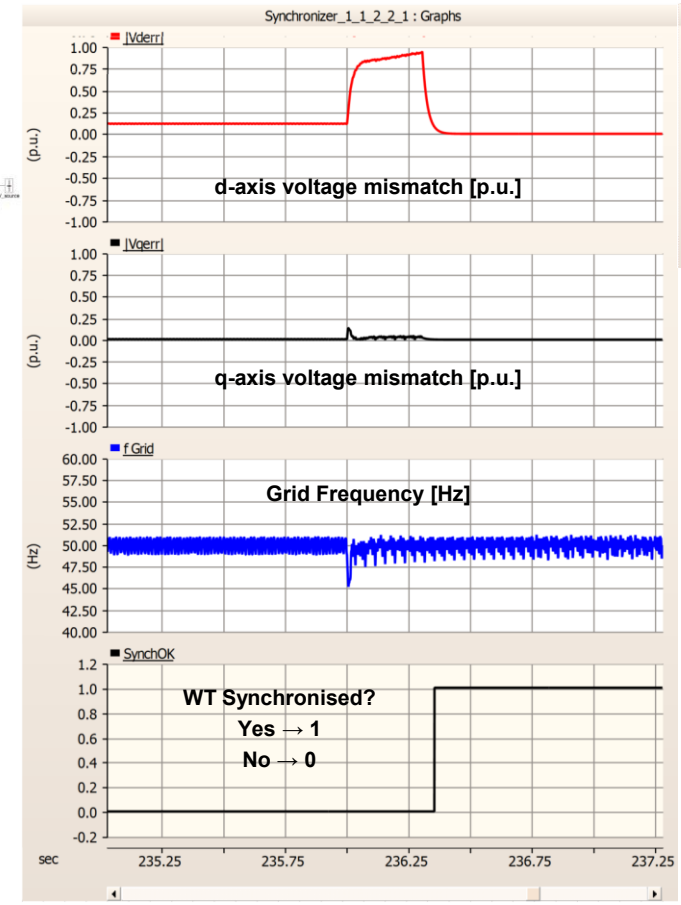


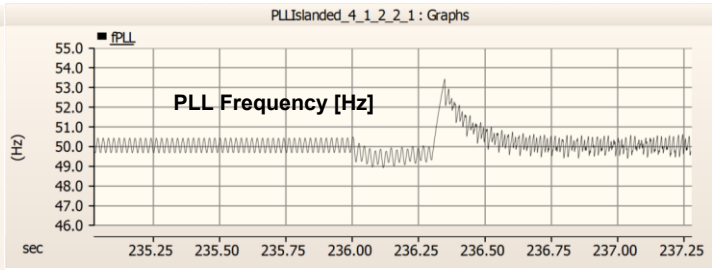


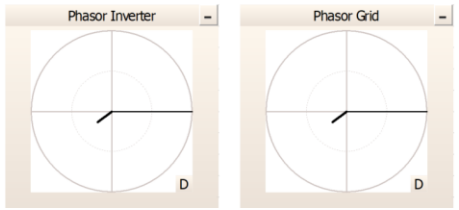
GFL WTGs Synchronisation

Single-string case at 4.5 m/s









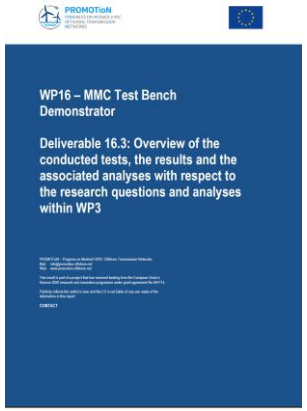
- WTG6 voltage mismatches converge towards zero following the event around 236 s.
- *SynchOK* confirms synchronization at approx. 236.36 s.
- Local PLL frequency peaks near 53.5 Hz and returns close to 50 Hz by approximately 236.8 s.
- Frequency estimates retain more ripple than in the mirrored two-string case.
- *SynchOK* asserts before full PLL recovery; confirm the subsequent breaker and deblocking sequence.

Research positioning

Low-wind self-start and GFL participation in context

Reference	What they demonstrate	What they did not demonstrate	What I can use	What my models already provide	Gap relevant to Journal 1
Huang et al., 2024	Power-speed limits, charging and converter limits, and GFM/GFL operation at 12 m/s.	Wind-driven acceleration from standstill to startup readiness at low wind.	Energy balance, charging and converter limits.	Explicit rotor acceleration with min speed interlock, (0.85 pu) followed by DC charging and collector energisation.	Reaching startup readiness from standstill at low wind.
PROMOTioN D16.3, 2020	Experimental soft energisation at 5 m/s, starting from idling, including auxiliaries.	Standstill startup followed by active follower participation in that experiment.	Experimental benchmark and auxiliary-demand treatment.	Startup from rest, 66 kV collector circuits and staged participation of 4 active followers.	Standstill startup followed by active GFL participation.
Zhang and Zhao, 2025	Wind-driven startup from standstill at 9–20 m/s; pitch and DC startup control.	Low-wind restoration combining GFM and GFL turbines.	DC startup sequence and Pitch control.	Individual GFM/GFL turbines; successful collector restoration at 4.5 m/s.	Low-wind restoration with individual GFM and GFL turbines.


Novel Black Start Control Strategy With Power Boundary Analysis for PMSG-Based Wind Turbines



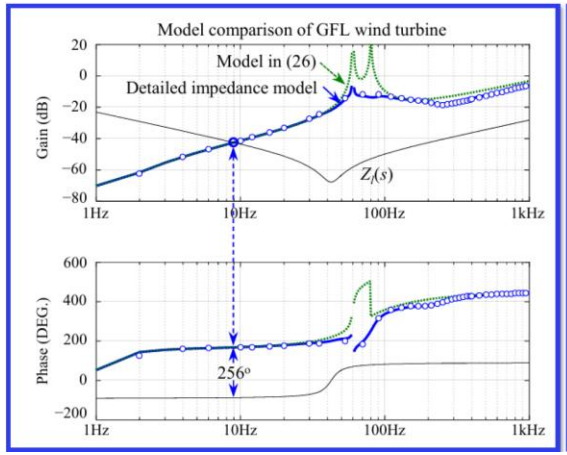

Startup Control of Grid-Forming Offshore Wind Turbines Connected to the Diode-Rectifier-Based HVDC Link

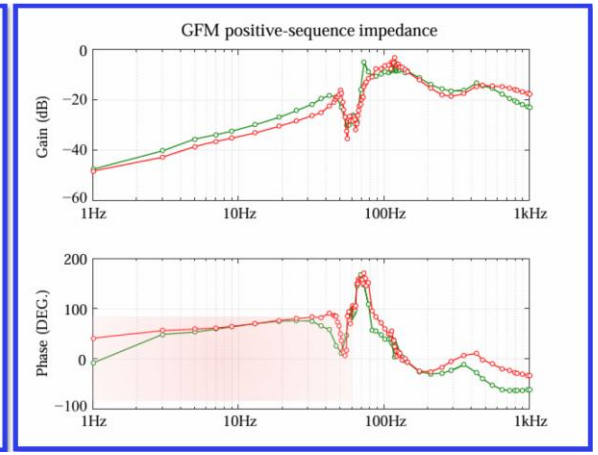
[8], [30], [31]

Diagnosing the converter–network interactions

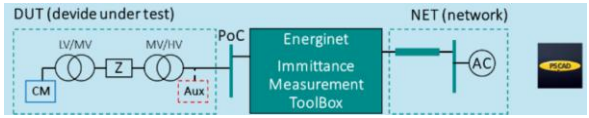
Impedance calculations

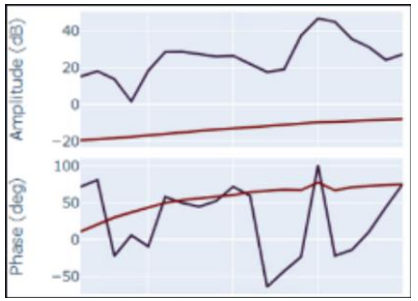
- Changing collector-cable parameters or variable wind destabilises the two-string benchmark.
- Obtain frequency responses from the PSCAD model (Energinet IMTB) and compare the cable configurations and use impedance-based stability analysis to identify possible corrective changes.
- Identify the critical converter–network interaction and test targeted control adjustments, starting from stable operating points.
- Participation Analysis and Admittance Matrix:
  - Identify which turbines contribute most to an oscillation and which control adjustments could help it die out.
  - Estimate how sensitive stable operation is to changes in connected equipment, highlighting vulnerable connection points and operating conditions.
  - Determine whether participation analysis or Admittance Margin adds useful diagnostic or robustness information.
- Validate the proposed correction by repeating the original blackstart sequence with the asymmetric collector cables.

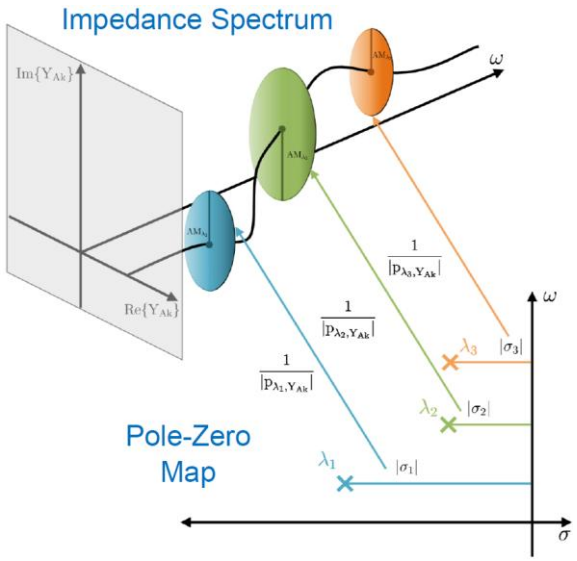




ENERGINET







[19], [32], [33]